Article

Cell Metabolism

GLP-1R Agonists Promote Normal and Neoplastic Intestinal Growth through Mechanisms Requiring *Fgf7*

Graphical Abstract

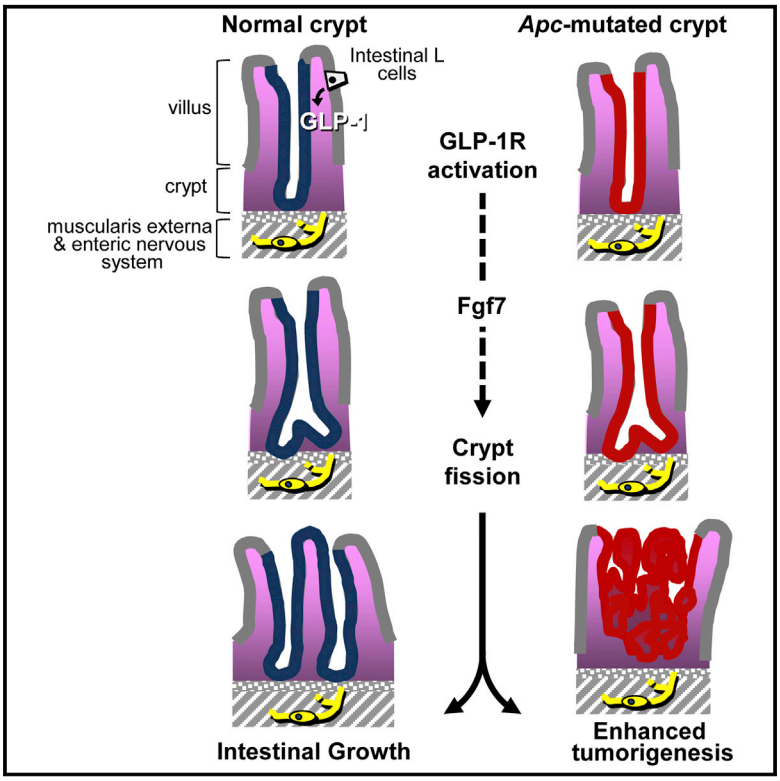

Highlights

- Activation of GLP-1 receptor signaling promotes gut growth and crypt fission
- Loss of GLP-1R signaling reduces growth in models of gut hyperplasia and tumorigenesis
- GLP-1R agonists promote small and large bowel growth via Fgf7

Authors

Jacqueline A. Koehler, Laurie L. Baggio, ..., Patricia L. Brubaker, Daniel J. Drucker

Correspondence

drucker@lunenfeld.ca

In Brief

Analogues of glucagon-like peptide-1 (GLP-1) are used to treat diabetes for their blood glucose lowering effects. Koehler et al. now show that GLP-1 also promotes gut growth through Fgf7 and that loss of GLP-1 signaling reduces growth in models of gut hyperplasia and tumorigenesis.

Accession Numbers

GSE63841

Koehler et al., 2015, Cell Metabolism *21*, 379–391
March 3, 2015
http://dx.doi.org/10.1016/j.cmet.2015.02.005

CellPress

Cell Metabolism
Article

GLP-1R Agonists Promote Normal and Neoplastic Intestinal Growth through Mechanisms Requiring *Fgf7*

Jacqueline A. Koehler,[1] Laurie L. Baggio,[1] Bernardo Yusta,[1] Christine Longuet,[1] Katherine J. Rowland,[2] Xiemin Cao,[1] Dianne Holland,[1] Patricia L. Brubaker,[2] and Daniel J. Drucker[1,*]
[1]Department of Medicine, Lunenfeld-Tanenbaum Research Institute, Mount Sinai Hospital, Toronto, ON M5G1X5, Canada
[2]Department of Physiology, University of Toronto, Toronto, ON M5S1A8, Canada
*Correspondence: drucker@lunenfeld.ca
http://dx.doi.org/10.1016/j.cmet.2015.02.005

SUMMARY

Glucagon-like peptide-1 (GLP-1) secreted from enteroendocrine L cells promotes nutrient disposal via the incretin effect. However, the majority of L cells are localized to the distal gut, suggesting additional biological roles for GLP-1. Here, we demonstrate that GLP-1 receptor (GLP-1R) signaling controls mucosal expansion of the small bowel (SB) and colon. These actions did not require the epidermal growth factor (EGF) or intestinal epithelial insulin-like growth factor (IGF1) receptors but were absent in *Glp1r*$^{-/-}$ mice. Polyp number and size were increased in SB of exendin-4-treated *Apc*$^{Min/+}$ mice, whereas polyp number was reduced in SB and colon of *Glp1r*$^{-/-}$:*Apc*$^{Min/+}$ mice. Exendin-4 increased fibroblast growth factor 7 *(Fgf7)* expression in colonic polyps of *Apc*$^{Min/+}$ mice and failed to increase intestinal growth in mice lacking *Fgf7*. Exogenous exendin-4 and Fgf7 regulated an overlapping set of genes important for intestinal growth. Thus, gain and loss of GLP-1R signaling regulates gut growth and intestinal tumorigenesis.

INTRODUCTION

Gut peptides act as circulating hormones or neurotransmitters to control appetite, gastrointestinal motility, gall bladder emptying, pancreatic enzyme secretion, and the absorption and disposal of ingested nutrients. The proglucagon-derived peptides (PGDPs), encompassing glicentin, oxyntomodulin, GLP-1, and glucagon-like peptide-2 (GLP-2), are among the best-studied products of the enteroendocrine L cell and regulate energy ingestion, absorption, and disposal (Campbell and Drucker, 2013; Drucker and Yusta, 2014). Analogues of GLP-1 and GLP-2 have been approved for the treatment of diabetes and short bowel syndrome, respectively, further highlighting conservation of key metabolic pathways linking gut peptide action to the control of energy homeostasis.

GLP-1 is classically viewed as an incretin that rapidly augments glucose-dependent insulin secretion following meal ingestion. GLP-1 also inhibits glucagon secretion, gastric emptying, and food intake, leading to reduction of glycemia and weight loss. Despite the distal location of most GLP-1-producing L cells in the ileum and colon, GLP-1 levels rise rapidly within minutes of meal ingestion, findings attributed to direct secretion from a subset of L cells in the jejunum and a proximal-distal neuroendocrine axis that communicates signals enabling secretion of PGDPs from the ileum and colon.

Several alternative explanations have arisen for the role and location of distal gut L cells. Colonic L cells may function as an energy sensor, secreting GLP-1 to modulate gut motility in response to fatty acids and energy availability (Wichmann et al., 2013). Alternatively, distal L cells may liberate GLP-1 in response to microbial byproducts (Molina et al., 2014), or other metabolites from digested nutrients (Reimann et al., 2012). A third role for GLP-1 in the distal gut includes stimulation of SB growth (Kissow et al., 2012; Simonsen et al., 2007); however, mechanisms linking GLP-1R signaling to augmentation of mucosal growth remain obscure.

Here, we demonstrate that gain and loss of GLP-1R signaling modulates intestinal growth in the SB and large bowel (LB). Intestinal growth in *Gcgr*$^{-/-}$ mice was differentially reduced in *Gcgr*$^{-/-}$:*Glp1r*$^{-/-}$ versus *Gcgr*$^{-/-}$:*Glp2r*$^{-/-}$ mice, whereas the intestinotrophic actions of exogenous GLP-1 and GLP-2 in wild-type (WT) mice were mediated by distinct mechanisms. The intestinotrophic actions of GLP-1R agonists did not require the EGF receptor or the intestinal epithelial IGF-1 receptor, but were mediated by GLP-1R-dependent stimulation of crypt fission through *Fgf7*-dependent mechanisms. Exendin-4 increased polyp size and number in *Apc*$^{Min/+}$ mice, a model of intestinal tumorigenesis, whereas polyp number was significantly reduced in *Glp1r*$^{-/-}$:*Apc*$^{Min/+}$ mice. These findings extend current concepts of GLP-1 action in the distal gut to encompass control of intestinal growth.

RESULTS

Endogenous GLP-1 and GLP-2 Independently Mediate Intestinal Growth

We first assessed whether endogenous native GLP-1, acting through the canonical GLP-1R, is capable of promoting bowel growth in *Gcgr*$^{-/-}$ mice that exhibit increased circulating levels of GLP-1 and GLP-2 (Ali et al., 2011; Gelling et al., 2003; Grigoryan et al., 2012). SB and LB mass and length were increased

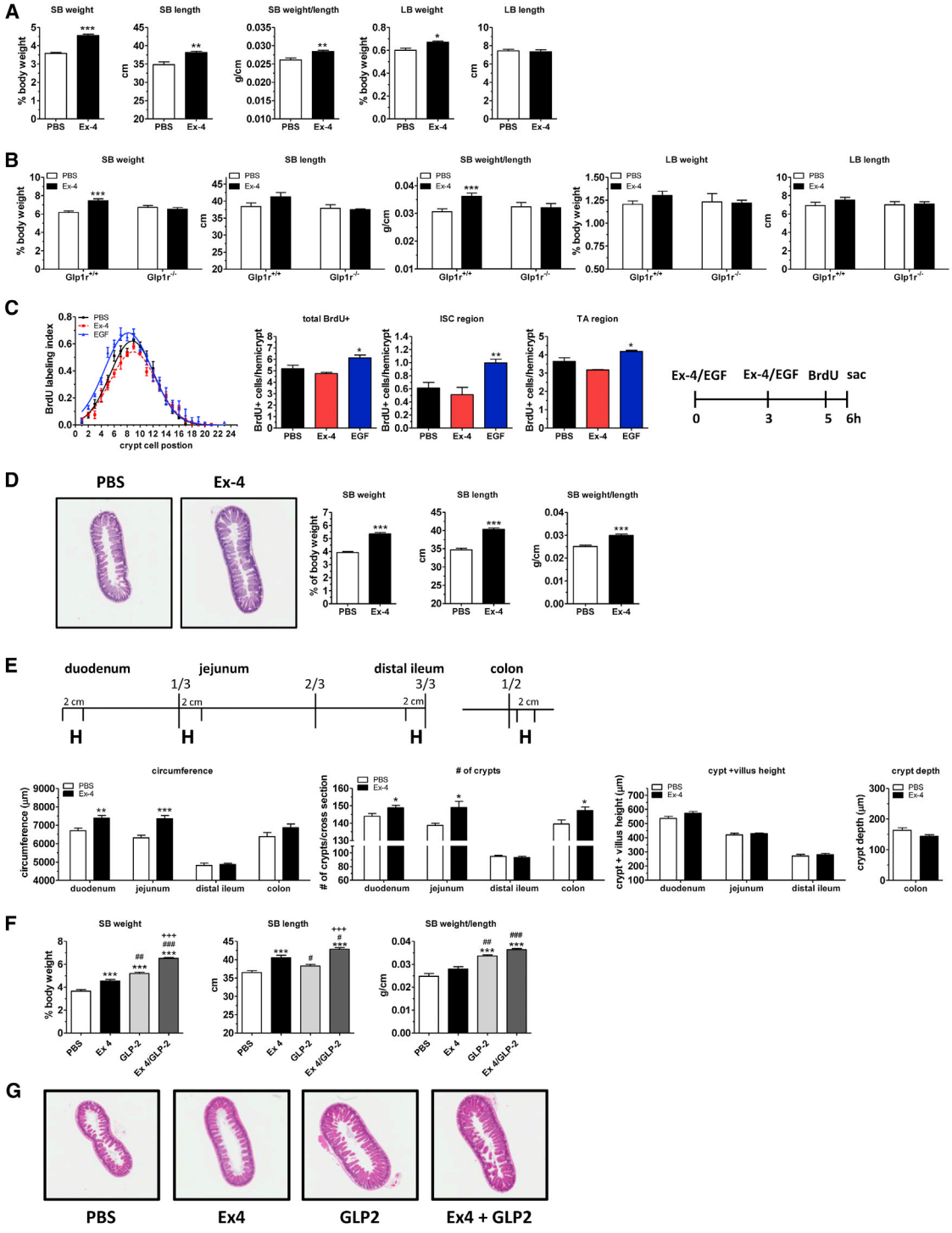

Figure 1. GLP-1R Activation Promotes Intestinal Growth by Increasing Crypt Number Rather than Augmenting Villus Length

(A) Small bowel (SB) and large bowel (LB) weight (as a percentage of body weight), length, and weight/unit length in C57BL/6 male mice following administration of Ex-4 or vehicle (PBS) for 7 days. n = 5 in each group.

(B) SB and LB weight (as a percentage of body weight) and length, and SB weight/unit length of female *Glp1r*$^{-/-}$ and *Glp1r*$^{+/+}$ littermate control mice administered Ex-4 or PBS for 10 days. n = 4–6 mice per group.

(C) BrdU labeling in the jejunal crypt compartment of WT mice treated with Ex-4, EGF, or PBS followed by a 1 hr pulse with BrdU. Schematic representation of the experimental design is shown (far right panel). Incidence of staining (BrdU labeling index) at each cell position within the crypt is shown (far left panel). Position 1 corresponds to the base of the crypt. Tissue sections were scored for total number of BrdU^{+} cells, BrdU^{+} cells in the intestinal stem cell (ISC) region (crypt base

(legend continued on next page)

in *Gcgr*$^{-/-}$ mice (Figures S1A and S1B), consistent with elevations in GLP-2, a peptide with known intestinotrophic activity (Drucker and Yusta, 2014; Gelling et al., 2003). Nevertheless, SB weight and length were reduced, but not normalized, while LB mass and length remained elevated in *Gcgr*$^{-/-}$*:Glp2r*$^{-/-}$ mice (Figure S1B). Elimination of the GLP-1R failed to normalize SB weight. However, SB length and LB weight and length were normalized in *Gcgr*$^{-/-}$*:Glp1r*$^{-/-}$ mice (Figure S1A). Hence, GLP-1R signaling independent of the GLP-2R mediates trophic effects predominantly in the distal gastrointestinal tract of *Gcgr*$^{-/-}$ mice.

GLP-1R Activation Promotes Intestinal Growth by Increasing Crypt Number

To identify mechanisms through which GLP-1R signaling promotes gut growth independent of confounding metabolic perturbations arising in *Gcgr*$^{-/-}$ mice (Gelling et al., 2003), we treated C57BL/6 WT mice with the clinically approved GLP-1R agonist exenatide (Ex-4: exendin-4) for 1 week. Ex-4 markedly increased the weight, length, and weight per unit length of the SB and significantly augmented LB weight (Figures 1A and S1C). Furthermore, the intestinotrophic effects of Ex-4 and a long-acting human GLP-1R agonist, liraglutide, were mediated through the GLP-1R, as they had no effect on bowel growth in *Glp1r*$^{-/-}$ mice (Figures 1B, S1D, and S1E). Although GLP-2 induces intestinal growth by increasing crypt cell proliferation (Drucker et al., 1996), Ex-4 did not enhance cell proliferation in the crypt compartment of the jejunum (Figure 1C) or colon (Figure S1F). In contrast, EGF increased the number of BrdU+ cells in the intestinal stem (ISC) region and in the transit amplifying (TA) region (Figure 1C), suggesting that GLP-1R signaling induces intestinotrophic effects through mechanisms that diverge from those activated by GLP-2 or EGF.

To determine whether the intestinotrophic actions of GLP-1R agonists are sustained with chronic administration, we treated mice with Ex-4 twice daily for 1 month. Ex-4 increased SB weight and length (Figures 1D and S1G) and increased the circumference and crypt number in the proximal (Figure 1E, *duodenum and jejunum*), but not the most distal region of the SB (Figure 1E, *distal ileum*). Similarly, Ex-4 significantly increased the number of crypts/cross-section in the colon (Figure 1E). In contrast, chronic Ex-4 treatment did not increase colon crypt depth or SB crypt + villus height (Figure 1E). These results suggest that sustained GLP-1R activation increases crypt number, but not crypt cell proliferation, to promote intestinal growth. Consistent with independent contributions of endogenous GLP-1 and GLP-2 on bowel growth in *Gcgr*$^{-/-}$ mice (Figures S1A and S1B), co-administration of the GLP-2R agonist h[Gly^2]GLP-2 (Drucker et al., 1997) and Ex-4 significantly increased SB weight and length to a greater extent than either peptide alone (Figures 1F and S1H). Furthermore, histological examination revealed that whereas jejunal circumference was increased by Ex-4, GLP-2 increased villus length (Figure 1G). Taken together, whereas GLP-2 promotes intestinal growth by inducing crypt cell proliferation and villus elongation (Drucker and Yusta, 2014), GLP-1R agonism promotes crypt fission and augments crypt number, resulting in an increase in the width and length of the intestine.

GLP-1R Signaling Controls Polyp Burden in *Apc*$^{Min/+}$ Mice

Subjects with obesity or type 2 diabetes exhibit increased rates of colon cancer (Calle and Thun, 2004; Lai et al., 2013; Li et al., 2011). Hence, we examined *GLP1R* expression in human colon tumors. The *GLP1R* (Figure 2A) and both the *GLP2R* and glucose-dependent insulinotropic polypeptide receptor (*GIPR*) mRNA transcripts (Figures S2A and S2B) were expressed in human colorectal tumors, but at lower levels relative to those in adjacent non-neoplastic colon samples from the same patients. *Glp1r* transcripts were also detected in colon polyps from *Apc*$^{Min/+}$ mice, a murine model of intestinal tumorigenesis (Figures 2B and S3E), at lower levels relative to normal adjacent colon or duodenum tissue (Figure 2B). Hence, the GLP-1R is not upregulated in benign or malignant intestinal lesions of epithelial origin. Nevertheless, Ex-4 significantly increased the number (Figures 2C and S3A) and size (Figures 2D and S3B) of polyps primarily in the distal SB of female (Figure 2) and male (Figure S3) *Apc*$^{Min/+}$ mice. In contrast, Ex-4 had no effect on polyp burden in more proximal regions of the SB or on the number or size of polyps or aberrant crypt foci (ACF) in the colon (Figures 2E, 2F, S3C, and S3D).

To examine the physiological importance of the endogenous GLP-1/GLP-1R system for polyp growth, we generated *Apc*$^{Min/+}$*:Glp1r*$^{-/-}$ mice. Strikingly, polyp burden was dramatically reduced in both female and male *Apc*$^{Min/+}$*:Glp1r*$^{-/-}$ mice. Loss of the *Glp1r* resulted in one-third fewer polyps throughout the entire SB (Figures 2G and S4A) without reducing polyp size (Figures 2H and S4B). Furthermore, significantly fewer polyps, but no differences in colonic ACFs or polyp diameter, were detected in the colons of *Apc*$^{Min/+}$*:Glp1r*$^{-/-}$ mice compared with *Apc*$^{Min/+}$*:Glp1r*$^{+/+}$ littermates (Figures 2I, 2J, S4C, and S4D). In addition, fewer *Apc*$^{Min/+}$*:Glp1r*$^{-/-}$ mice developed colon polyps (5 of 9 females and 9 of 11 males), whereas all *Apc*$^{Min/+}$*:Glp1r*$^{+/+}$

columnar cells [CBCs] + '4+' ISCs cells), and BrdU$^+$ cells in the transit amplifying (TA) region (positions 6–11) per hemicrypt, as indicated. n = 6 mice per group from two experiments.

(D and E) WT male mice were administered exogenous Ex-4 or PBS for 4 weeks. (D) Representative histological sections of jejunum stained with H&E from mice treated with PBS or Ex-4 for 4 weeks (left panels, magnification ×40), and SB weight (as a percentage of body weight), length, and weight/unit length (right panels). n = 10 in each group from three experiments. (E) Circumference surrounding the mucosa, number of crypts/cross section, and crypt + villus height (for SB), or crypt depth (for colon) are shown for each section of intestine as indicated. Schematic representation of the locations of the sections used for histology (H) is depicted above the data. n = 6–7 mice in each group.

(F) SB weight (as a percentage of body weight), length, and weight/unit length in C57BL/6 male mice following administration of PBS, Ex-4, Gly2-GLP-2 (GLP-2), or both Ex-4 and Gly2-GLP-2 (Ex-4/GLP-2) for 10 days. n = 5 in each group.

(G) Representative histological sections of jejunum stained with H&E from mice treated with PBS, Ex-4, Gly2-GLP-2 (GLP2), or both, as indicated. n = 5 in each group. Magnification ×40.

For (A)–(F), data are means ± SE. *p < 0.05, **p < 0.01, ***p < 0.001 versus PBS. #p < 0.05, ##p < 0.01, ###p < 0.001 Ex-4 versus h[Gly^2]GLP-2, or Ex-4+h[Gly^2]GLP-2; +++p < 0.001 h[Gly^2]GLP-2 versus Ex-4+ h[Gly^2]GLP-2. See also Figure S1.

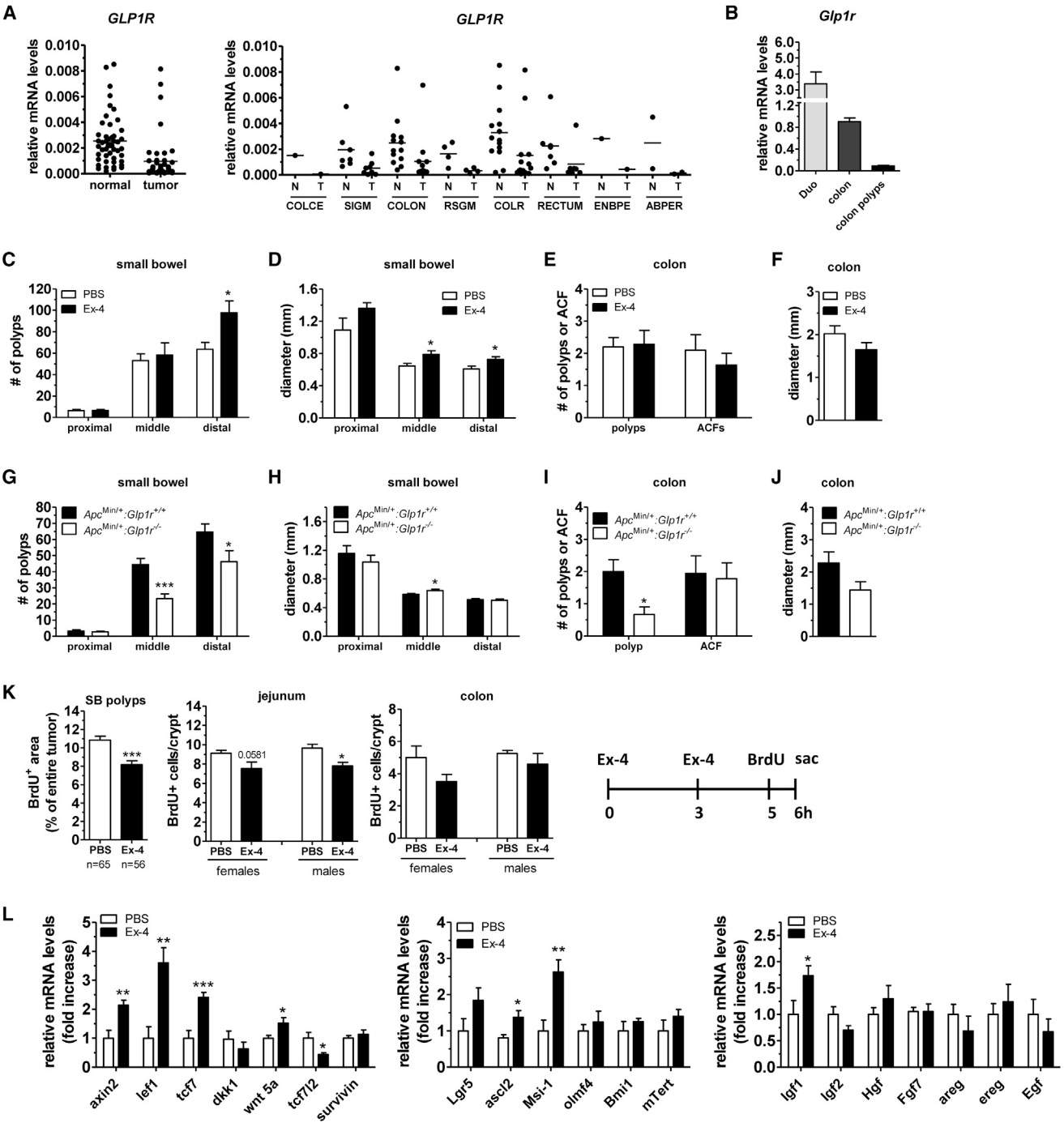

Figure 2. GLP-1R Signaling Modulates Polyp Burden in $Apc^{Min/+}$ Mice

(A) *GLP1R* expression by qPCR analysis of RNA samples from paired normal human colon or colonic adenocarcinoma. Left panel: relative *GLP1R* mRNA levels of all 50 normal human and tumor samples. Right panel: relative mRNA levels of normal colon (N) and tumor (T) samples designated and graphed according to tumor location. Colce (colon/cecum-proximal colon), SGM (sigmoid colon-distal region before rectum), Colon, RSGM (rectosigmoid), COLR (colorectal), Rectum, ENBPE (en-bloc peritoneum), ABPER (abdominal peritoneal).

(B) *Glp1r* expression by qPCR analysis of normal (i.e., without polyps) duodenum (Duo), colon, or colon polyps of $Apc^{Min/+}$ mice. Data are means ± SE, n = 10 mice per group.

(C–F) $Apc^{Min/+}$ mice were administered Ex-4 or PBS for 4 weeks. Number (C) and size (D) of polyps in regions of the small bowel of female $Apc^{Min/+}$ mice. Number of polyps and aberrant crypt foci (ACF) (E) and size of polyps (F) in colons of female $Apc^{Min/+}$ mice. n = 9 per group. Data are means ± SE. *p < 0.05 versus PBS.

(G–J) Number (G) and size (H) of polyps in regions of the SB of female $Apc^{Min/+}$:$Glp1r^{+/+}$ and littermate $Apc^{Min/+}$:$Glp1r^{-/-}$ mice. The number of polyps and ACFs (I) and size of polyps (J) in the colons of female $Apc^{Min/+}$:$Glp1r^{+/+}$ and littermate $Apc^{Min/+}$:$Glp1r^{-/-}$ mice. n = 9 for all genotypes. Data are means ± SE. *p < 0.05, ***p < 0.001 $Apc^{Min/+}$:$Glp1r^{+/+}$ versus $Apc^{Min/+}$:$Glp1r^{-/-}$ mice.

(legend continued on next page)

mice (9 females and 11 males) developed at least one colon polyp. Taken together, these results demonstrate that gain or loss of GLP-1R signaling modifies the number of intestinal polyps in $Apc^{Min/+}$ mice.

Although GLP-2 stimulates cell proliferation (Drucker et al., 1996), acute Ex-4 administration reduced cell proliferation in SB polyps and decreased basal crypt cell proliferation in the jejunum, but not the colon, of $Apc^{Min/+}$ mice (Figure 2K). In contrast, chronic Ex-4 treatment reduced the number of apoptotic cells but had no effect on neutrophil infiltration in SB polyps (Figures S3F and S3G). Acute Ex-4 administration increased the phosphorylation/inactivation of GSK3 in colonic polyps (Figure S3H), whereas chronic Ex-4 treatment increased expression of Wnt target genes (*axin2*, *lef1*, *tcf7*) and the ligand *Wnt5a* in colon polyps of $Apc^{Min/+}$ mice (Figure 2L). Moreover, levels of mRNA transcripts encoding the ISC markers musashi-1 (*msi-1*) and achaete-scute complex-like-2 (*ascl2*) were upregulated in colon polyps of chronically Ex-4-treated $Apc^{Min/+}$ mice (Figure 2L) as well as in the jejunum of C57BL/6 mice upon chronic Ex-4 exposure (Figure S5A). Examination of growth factor receptor and ligand expression (Figures 2L and S3I) revealed upregulation of *Igf1* mRNA transcripts in colonic polyps of chronically Ex-4-treated $Apc^{Min/+}$ mice. In contrast, loss of GLP-1R signaling did not reveal significant changes in expression of candidate growth-regulating genes (Figure S4E) or signaling pathways (Figure S4F) in colonic polyps of $Apc^{Min/+}$:$Glp1r^{-/-}$ mice.

Epithelial IGF1 or EGF Receptor Signaling Pathways Are Not Essential for GLP-1R-Mediated Intestinal Growth

A summary of selected gene expression profiles in the intestine of Ex-4-treated mice is shown in Table S1. Ex-4 upregulated *Igf1* transcripts in the jejunum and colon and *areg* and *ereg* in the jejunum of C57BL/6 mice (Figure 3A) as well as *Igf1r* and *areg* in the duodenum of WT (Figure S5C) and $Apc^{Min/+}$ mice (Table S1). Ex-4 also acutely induced *ereg* mRNA levels in colon polyps of $Apc^{Min/+}$ mice (Figure 3B) as well as *tcf7* and *tcf7l2* transcripts in the jejunum of C57BL/6 mice (Figure S5B). These findings suggested that GLP-1R activation may induce receptor tyrosine kinase IGF1R/ErbB(EGFR) (*igf1*, *areg*, *ereg*) pathways to regulate intestinal growth and tumorigenesis. We therefore examined whether the intestinal growth-promoting effects of Ex-4 or liraglutide were preserved in (i) mice with a conditional deletion of the IGF-1R from intestinal epithelial cells (IE-*Igf1r*KO) (Rowland et al., 2011) and (ii) $Egfr^{wa2/wa2}$ (*waved*) mice harboring a loss-of-function point mutation in the EGFR kinase domain (Luetteke et al., 1994). Liraglutide increased SB weight and length in IE-*Igf1r*KO mice, and colon weight trended higher in liraglutide-treated IE-*Igf1r*KO and littermate control mice (Figure 3C). Ex-4 also increased SB weight, and colon weight trended higher after Ex-4 in $Egfr^{wa2/wa2}$ and heterozygote littermate controls (Figure 3D). Hence, GLP-1R agonists induce components of IGF-1 and ErbB signaling pathways. However, intestinal epithelial IGF1 or EGF receptor signaling is not essential for GLP-1R-mediated induction of intestinal growth.

Fgf7 Is Required for GLP-1R-Mediated Intestinal Growth

As the intestinotrophic actions of GLP-2 in the mouse colon, but not the small bowel, are attenuated by immunoneutralization of keratinocyte growth factor (KGF) (Ørskov et al., 2005), we examined whether KGF, encoded by the *Fgf7* gene, plays a role in the intestinotrophic effects of GLP-1R agonists. Although Ex-4 administration did not induce *Fgf7* expression in the colon of C57BL/6 mice (Figure S5E) or in the jejunum after chronic administration (Figure S5D), Ex-4 acutely increased *Fgf7* mRNA levels in the small bowel of WT mice (Figure 4A) and in colon polyps of $Apc^{Min/+}$ mice (Figure 4B). Strikingly, the intestinotrophic effects of Ex-4 were abolished in $Fgf7^{-/-}$ mice (Figures 4C, S6A, and S6B). The inability of Ex-4 to increase bowel growth in $Fgf7^{-/-}$ mice was not due to defective *Glp1r* expression, as levels of intestinal *Glp1r* mRNA transcripts were similar in $Fgf7^{-/-}$ versus littermate control mice (Figure 4G). Furthermore, the intestinal growth factors GLP-2 (Figures 4D and S6C) and EGF (Figures 4E and S6D) robustly increased SB and LB weight in both $Fgf7^{-/-}$ and littermate control mice. Moreover, classical metabolic and motility actions of GLP-1R agonists were preserved in $Fgf7^{-/-}$ mice (Figures 4F and S6E). Hence, $Fgf7^{-/-}$ mice do not exhibit a generalized resistance to intestinal growth factors or GLP-1R agonists; however, the intestinal growth-promoting actions of GLP-1R agonists are selectively mediated through mechanisms requiring *Fgf7*.

Fgf7 was expressed in colon and upregulated in colonic polyps of $Apc^{Min/+}$ mice; expression of the receptor for Fgf7, *Fgfr2IIIb*, was also detected in RNA from colon and colonic polyps, and both *FGF7* and *FGFR2* mRNA transcripts were detected in RNA from normal colon and human colonic adenocarcinoma (Figures 4H and 4I), in agreement with previous analyses (Otte et al., 2000). These experiments suggest that enhanced or disrupted GLP-1R signaling modifies normal and neoplastic intestinal growth via a GLP-1R-*Fgf7* axis.

Overlapping Intestinal Gene Expression Profiles Regulated by Ex-4 and Fgf7/Kgf

To identify growth-related signaling pathways activated by GLP-1R agonists and/or Fgf7 in the gut, we carried out microarray (Illumina WG-6) analysis on jejunal RNA prepared from mice 1 hr, 5 hr, and 20 hr following a single dose of Ex-4 or Fgf7. The number of genes significantly upregulated or downregulated at least 1.2-fold by Ex-4 or Fgf7 is shown in Figure 5A. Real-time PCR independently verified that several genes were regulated by both Ex-4 and Fgf7, including *phlda1* (pleckstrin homology-like domain, family A, member 1), *asns* (asparagine synthetase), *pcsk9* (proprotein convertase subtilisin/kexin type 9), *mthfd2* (methylenetetrahydrofolate dehydrogenase [NAD+ dependent]),

(K) BrdU incorporation in SB polyps and in jejunal and colon crypt compartments of $Apc^{Min/+}$ mice treated with Ex-4 or PBS. Schematic representation of the experimental design is shown (right panel). For SB polyps, BrdU+ area is shown as the percentage of the total area of the polyp. n = number of polyps quantified from 6 mice. For the jejunum and colon, tissue sections were scored for total number of BrdU+ cells per crypt. n = 6 mice in each group. Data are means ± SE. *$p < 0.05$, ***$p < 0.001$ versus PBS.

(L) qPCR analysis of colon polyps of $Apc^{Min/+}$ mice treated with PBS or Ex-4 for 4 weeks. n = 5 or 8 in each group. Data are means ± SE from three experiments. *$p < 0.05$, **$p < 0.01$, ***$p < 0.001$ versus PBS. See also Figures S2–S4 and Table S1.

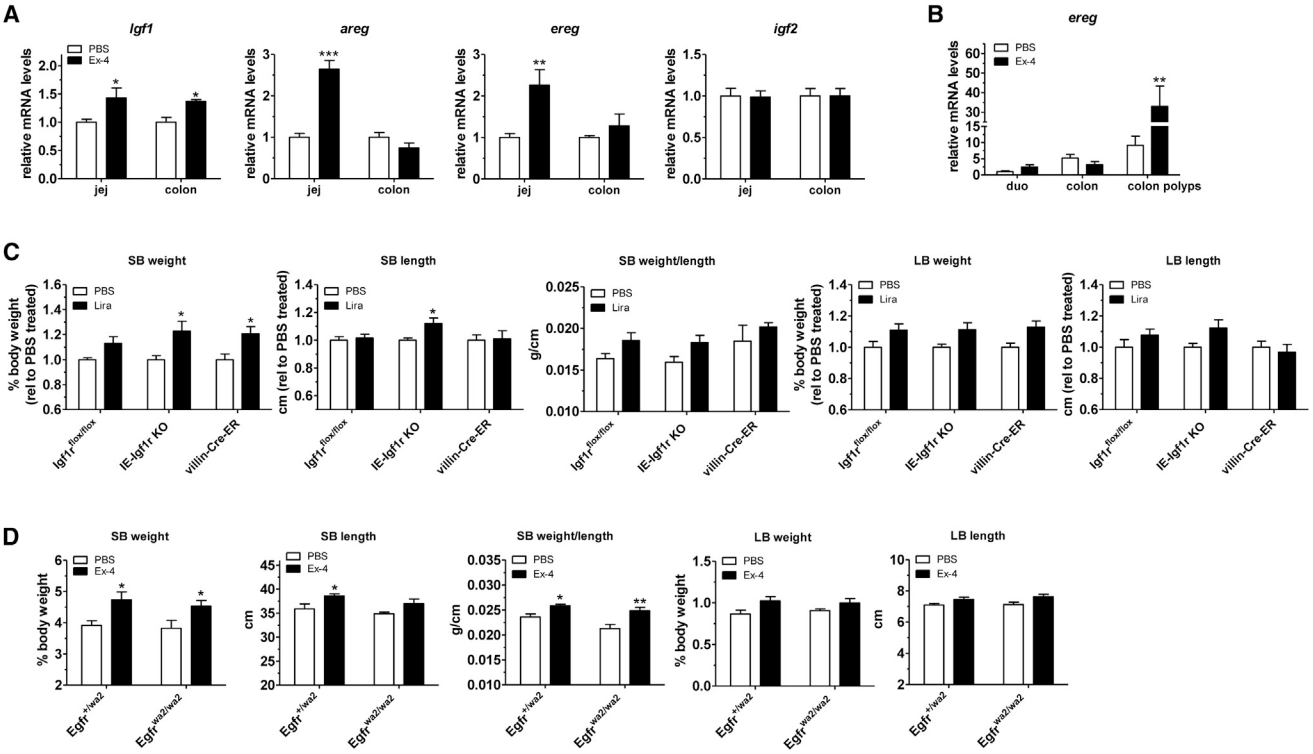

Figure 3. IGF1R/EGFR Signaling Is Not Essential for the Intestinal Trophic Effects of GLP-1R Agonists

(A and B) qPCR analysis of RNA from jejunum and colon of C57BL/6 mice 4 hr after a single injection with Ex-4 or PBS (n = 5 per group) (A) or normal (polyp-free) duodenum and colon, or colon polyps of *Apc*$^{Min/+}$ mice 30 min after injection of Ex-4 or PBS (n = 4–5 mice per group) (B). Data are means ± SE. *p < 0.05, **p < 0.01, ***p < 0.001 versus PBS.

(C) Small bowel (SB) and large bowel (LB) weight (as a percentage of body weight and relative to PBS-treated controls), length (relative to PBS-treated controls), and SB weight/unit length of *Igf1r*$^{flox/flox}$, *IE-Igf1r* KO, and *villin-Cre-ER*$^{T2+/0}$ mice treated with PBS or liraglutide for 8 days. n = 4–6 mice per group. Data are expressed relative to the respective PBS-treated controls of males and females combined and are expressed as means ± SE. *p < 0.05 versus PBS.

(D) SB and LB weight (as a percentage of body weight), length, and SB weight/unit length of female *Egfr*$^{+/wa2}$ and *Egfr*$^{wa2/wa2}$ mice treated with Ex-4 or PBS for 7 days. n = 5 (PBS) or n = 6 (Ex-4) mice for each genotype. Data are means ± SE from two experiments. *p < 0.05, **p < 0.01 versus PBS. See also Figure S5 and Table S1.

fkbp11 (FK506 binding protein 11), *gar1* (GAR1 ribonucleoprotein homolog), and *adck5* (aarF domain containing kinase 5) (Figure 5B). In contrast, Fgf7, but not Ex-4, induced the expression of *egr-1* (early growth response 1) and *tff2* (trefoil factor 2), whereas Ex-4, but not Fgf7, upregulated levels of *mmp13* (matrix metallopeptidase 13) and *Reg3b* (regenerating islet-derived protein III beta) RNA transcripts (Figure 5B). Notably, several genes induced by both Ex-4 and Fgf7, including *phlda1* (Sakthianandeswaren et al., 2011), *asns* (Zhang et al., 2014), and *mthfd2* (Nilsson et al., 2014), encode proteins important for regulation of cell proliferation, migration, or survival.

Ex-4 Does Not Increase Intestinal Weight in *Glp1r*$^{-/-}$ Mice Reconstituted with *Glp1r*$^{+/+}$ Intestinal Intraepithelial Lymphocytes

The *Glp1r* is expressed in murine intestinal intraepithelial lymphocytes (IELs) (http://www.immgen.org; B.Y. and D.J.D., unpublished data), and Tγδ IELs have been implicated in repair of the intestinal mucosa through Fgf7/KGF (Boismenu and Havran, 1994; Chen et al., 2002). To address whether IELs link GLP-1R signaling to Fgf7 expression and gut growth, we generated bone marrow chimeras by reconstituting lethally irradiated *Glp1r*$^{+/+}$ and *Glp1r*$^{-/-}$ mice with congenic bone marrow from *Glp1r*$^{+/+}$ donor mice. Donor chimerism, determined by flow cytometry 14–16 weeks after transplant, was 95.9% ± 0.8% and 80.8% ± 4.6% in spleen and purified small intestinal IELs from recipient mice, respectively (Figure 6A). Analysis of *Glp1r* expression independently confirmed that IELs derived from transplanted marrow repopulated the intestinal compartment (Figure 6B). The reconstitution efficiency of *Glp1r* expression in the jejunum and purified IELs of *Glp1r*$^{-/-}$ recipients was 75% ± 21.4% and 90.7% ± 22.9%, respectively (Figure 6B). Nevertheless, Ex-4 did not induce intestinal growth in *Glp1r*$^{-/-}$ recipient mice, despite efficient reconstitution of *Glp1r*$^{+/+}$ IELs into *Glp1r*$^{-/-}$ recipient mice (Figure 6C). Furthermore, levels of *Fgf7* mRNA transcripts were extremely low (~1,000-fold lower than *Glp1r*) in sorted small intestinal IELs (>98% purity), even following in vitro activation (data not shown). In contrast, *Fgf7* mRNA transcripts were enriched in RNA from primary SB myofibroblast cultures, compared with RNA isolated from jejunum (Figure 6D). Although we detected a gene expression profile consistent with that previously reported for myofibroblasts in RNA from these cultures (Figure 6D), *Glp1r* mRNA transcripts were not expressed at significant levels. Hence, although Fgf7+ myofibroblasts remain a potential downstream target for GLP-1R-dependent control of gut growth, it seems likely that

one or more additional GLP-1R+ cell types, perhaps enteric neurons, are important for conveying GLP-1R-activated signals to Fgf7-dependent stimulation of intestinal growth.

DISCUSSION

Although pharmacological administration of GLP-1R agonists increased the mass of the rodent SB epithelium, mechanisms connecting GLP-1R activation to intestinal growth were not identified (Kissow et al., 2012; Simonsen et al., 2007). We demonstrate that enhanced GLP-1R signaling in *Gcgr*$^{-/-}$ mice also mediates intestinotrophic activity not only in the SB, but also in the colon. Importantly, increased colonic growth and SB length evident in *Gcgr*$^{-/-}$ mice were completely normalized in *Gcgr*$^{-/-}$*:Glp1r*$^{-/-}$ mice. The complementary effects of endogenous native GLP-1 and GLP-2 on gut growth in *Gcgr*$^{-/-}$ mice are supported by our demonstration that exogenous Ex-4 and h[Gly^2]GLP-2 produce additive effects on SB weight and length in WT mice. Hence, evidence from pharmacological peptide administration and genetic disruption of PGDP receptors is consistent with independent intestinotrophic actions of GLP-1 and GLP-2 through distinct mechanisms.

Our studies using gain and loss of GLP-1R signaling in *Apc*$^{Min/+}$ mice reveal the importance of the GLP-1R as a modifier of polyp size and number in a genetic model of intestinal tumor growth. Surprisingly, GLP-1R agonists did not increase crypt cell proliferation; rather, they expanded the mass of the epithelium through stimulation of crypt fission. Although mechanism(s) regulating crypt division/fission are not well defined, intestinal mucosal growth primarily occurs via crypt division in neonatal humans and rodents, whereas crypt fission occurs at very low rates in normal adult tissue. In contrast, crypt fission is induced in the adult intestine as part of the regenerative process following intestinal damage, including ulcerative colitis, surgical resection, or irradiation (Plamboeck et al., 2013a). Moreover, acquisition of a single *Apc*-deficient crypt is not sufficient to promote tumorigenesis, but rather a 'field' of adjacent mutated crypts, arising through crypt fission or independent neighboring events, is necessary for tumor initiation (Ali et al., 2015; Plamboeck et al., 2013b). Furthermore, intestinal crypts harboring oncogenic mutations can further expand through enhanced crypt fission in both the murine (Snippert et al., 2014) and human (Greaves et al., 2006) intestine. Taken together, our findings demonstrating that GLP-1R activation increases crypt number in WT mice and polyp burden in *Apc*$^{Min/+}$ mice support the concept that GLP-1/GLP-1R signaling regulates normal and neoplastic intestinal growth through modulation of crypt fission.

Although GLP-1R agonists induce molecular components of the IGF1R and ErbB signaling pathways in the murine gut, and GLP-2R signaling promotes growth via a combination of Igf1r- and ErbB-dependent pathways (Dubé et al., 2006; Yusta et al., 2009), disruption of intestinal epithelial IGF1R activity did not abrogate the GLP-1R-dependent stimulation of intestinal growth. Similarly, GLP-1R agonists augmented gut growth in *Egfr*$^{wa2/wa2}$ mice. Although insulin may potentially augment intestinal growth, we did not detect increased intestinal mass following administration of GLP-1R agonists to mice with normalization of GLP-1R-dependent insulin secretion (Lamont et al., 2012). In contrast, although GLP-1R agonists lowered glucose and inhibited gastric emptying in *Fgf7*$^{-/-}$ mice, activation of GLP-1R signaling failed to increase SB or LB mass in the absence of Fgf7. Furthermore, pharmacological administration of Fgf7 increases plasma levels of the PGDPs, including GLP-1, in rats (Goodlad et al., 2000), and FGF7 has been localized to the enteric nervous system in the human colon (Rodriguez-Diaz et al., 2011), providing further evidence for the existence of a Fgf7-L cell axis.

The essential role of Fgf7-dependent pathways in control of intestinal growth is further emphasized by findings that chemical inhibition of Fgfr2IIIb signaling significantly reduced intestinal polyp growth in *Apc*$^{Min/+}$ mice (Pathuri et al., 2014). FGF7 and its receptor FGFR2 are also expressed in human colon cancer (Otte et al., 2000; Watanabe et al., 2000; Yoshino et al., 2005), and increased *FGFR2* expression in human colorectal cancer correlated with more extensive disease, poor response to treatment, and reduced survival (Li et al., 2014). Conversely, reduction of *FGFR2* expression attenuates growth of human colon cancer cells in vitro (Matsuda et al., 2011).

Complementary evidence for a subset of pathways regulated by both GLP-1R agonists and Fgf7 derives from microarray and gene expression studies, which identified intestinal genes co-regulated by Fgf7 and Ex-4. We pursued the possibility that *Glp1r* expression in IELs may liberate Fgf7, which in turn promotes gut growth. Nevertheless, we were unable to restore GLP-1R-dependent intestinal growth following reconstitution of GLP-1R+ IELs in *Glp1r*$^{-/-}$ mice. Although limitations in the sensitivity and specificity of reagents for detection of the murine GLP-1R (Panjwani et al., 2013) and Fgf7 proteins limit current efforts to more precisely localize cell types linking GLP-1R signaling to Fgf7-dependent stimulation of gut growth, we did observe *Fgf7* expression in mouse SB myofibroblasts, whereas levels of *Glp1r* mRNA transcripts were barely detectable in SB myofibroblast RNA.

The GLP-1R has been localized to the enteric nervous system (ENS) in mice (Richards et al., 2014) and primates (Pyke et al., 2014), and FGF7 has been detected in the human ENS, raising the possibility that the ENS communicates a GLP-1R-dependent signal that converges on Fgf7 and ultimately promotes crypt fission. Although acute activation of GLP-1R signaling in enteric neurons rapidly propagates a signal to the intestinal mucosal epithelium, the precise downstream effectors of these signals remain unclear (Kedees et al., 2013). Similarly, the specific cell types and molecular mediators connecting intestinal GLP-1R signaling to Fgf7 and crypt fission require further clarification.

The demonstration that the *Fgf7*/*Fgfr2* axis is an important target for the intestinotrophic actions of GLP-1R agonists raises questions with translational implications. Although human subjects with type 2 diabetes and obesity exhibit increased rates of multiple cancers, incretin-based therapies have not been reported to increase cancer incidence, and GLP-1R agonists frequently produce weight loss, which may reduce the incidence of cancer (Ashrafian et al., 2011; Terzić et al., 2010). Whether long-term use of GLP-1R agonists will modify cancer risk in obese and/or diabetic subjects is unknown and will require analysis of large numbers of treated subjects, likely from registry studies.

Following bariatric surgery or genetic reduction of Gcgr signaling, levels of GLP-1, GLP-2, and bile acids are increased (Madsbad et al., 2014). Combined use of GLP-1 and GLP-2R

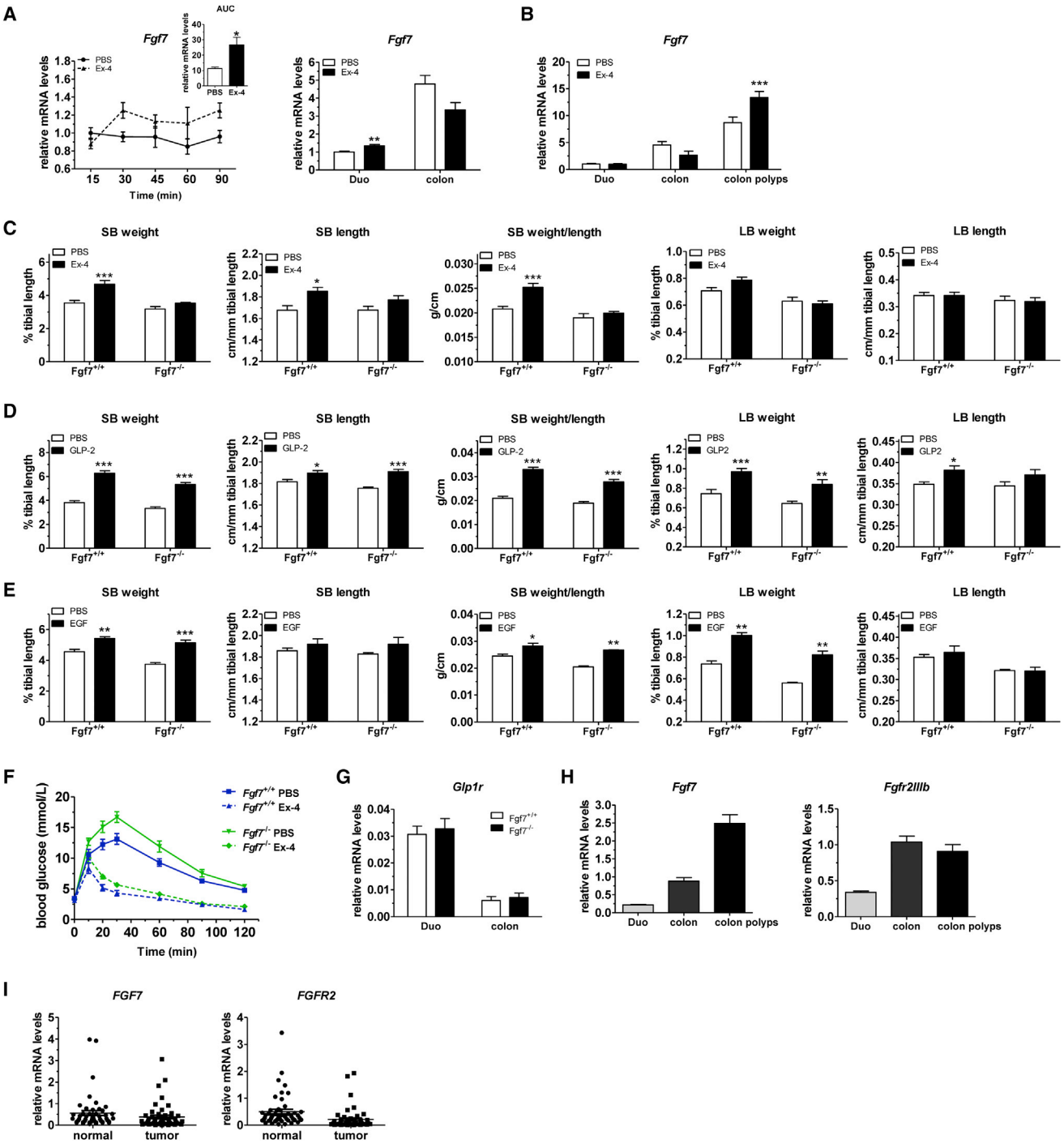

Figure 4. GLP-1R-Mediated Intestinal Growth Is Not Observed in *Fgf7*$^{-/-}$ Mice

(A) qPCR analysis of RNA isolated from jejunum of C57BL/6 mice 15–90 min after a single injection of Ex-4 or PBS (left panel). n = 4 male mice per group. Differences in mRNA levels of *Fgf7* were quantified by comparing the total AUC from 15–90 min in jejunum (inset, left panel) or from duodenum (Duo) and colon of WT littermates of *Apc*$^{Min/+}$ mice 6 hr after injection with Ex-4 or PBS (right panel). n = 6 in each group.

(B) qPCR analysis of RNA isolated from normal (polyp-free) duodenum (Duo) or colon or colon polyps of *Apc*$^{Min/+}$ mice 30 min after injection with Ex-4 or PBS. n = 5 (Duo and colon) or n = 4 (colon polyps) mice per group.

For (A) and (B), data are means ± SE. *p < 0.05, **p < 0.01, ***p < 0.001 versus PBS.

(C–E) Small bowel (SB) and large bowel (LB) weight (as a percentage of tibia length), length (relative to tibia length), and SB weight/unit length of *Fgf7*$^{+/+}$ or *Fgf7*$^{-/-}$ mice treated for 10 days with PBS or (C) Ex-4 (n = 6–8 females per group), (D) Gly2-GLP-2 (n = 5–6 females per group), or (E) EGF (n = 3–4 males per group). Data are means ± SE. *p < 0.05, **p < 0.01, ***p < 0.001 versus PBS.

(F) Intraperitoneal glucose tolerance test in *Fgf7*$^{+/+}$ and *Fgf7*$^{-/-}$ mice treated with PBS or Ex-4. n = 6 *Fgf7*$^{-/-}$ and n = 10 *Fgf7*$^{+/+}$ mice in each group.

(legend continued on next page)

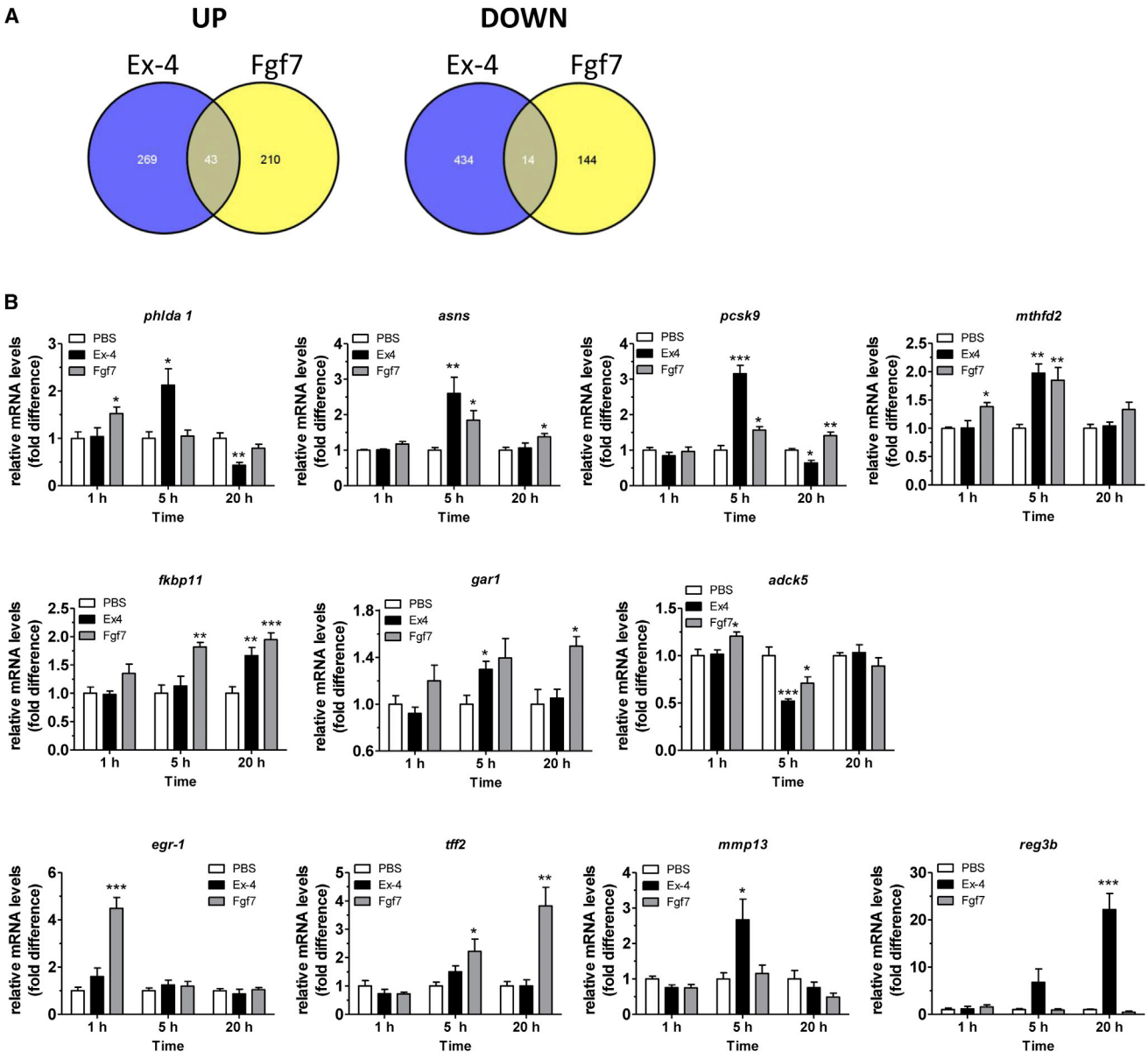

Figure 5. Intestinal Gene Expression Regulated by Both Ex-4 and Fgf7

(A) Venn diagrams summarizing the number of post hoc significant false discovery rate (FDR) corrected probes from the Illumina Mouse Whole Genome (WG-6V2) Beadchip microarray analyses that were significantly upregulated (UP) or downregulated (DOWN) by at least 1.2-fold relative to control-treated mice following treatment with Ex-4 or Fgf7 (KGF) from all 3 time points (1, 5, and 20 hr). 1 hr, n = 3; 5 hr, n = 4; 20 hr, n = 3.

(B) qPCR analysis of RNA isolated from jejunum of C57BL/6 mice 1 hr, 5 hr, or 20 hr after a single injection of Ex-4, Fgf7, or PBS. n = 5 male mice per group, from three independent experiments. Data are means ± SE. *p < 0.05, **p < 0.01, ***p < 0.001 versus PBS.

agonists for the treatment of short bowel syndrome has also been examined (Madsen et al., 2013). Although weight loss and bariatric surgery are generally associated with reduced rates of cancer (Sjöström et al., 2009), increased rates of colorectal cell proliferation and crypt fission have been detected in rectal mucosal biopsies from obese subjects as long as 3 years after bariatric surgery (Kant et al., 2011). Furthermore, a large nationwide retrospective cohort study of 15,905 obese subjects

(G) qPCR analysis of *Glp1r* mRNA expression in the duodenum (Duo) and colon of $Fgf7^{+/+}$ and $Fgf7^{-/-}$ mice. n = 5 mice per group.

(H) *Fgf7* and *Fgfr2IIIb* expression by qPCR analysis from normal (i.e., without polyps) duodenum (Duo), colon, or colon polyps of $Apc^{Min/+}$ mice. Data are means ± SE and are shown relative to colon. n = 5–6 mice per group.

(I) *FGF7* and *FGFR2* expression by qPCR analysis of RNA samples from paired normal human colon or colonic adenocarcinoma. Shown are relative mRNA levels of all 50 human tumor and normal samples analyzed in one experiment. See also Figures S5 and S6 and Table S1.

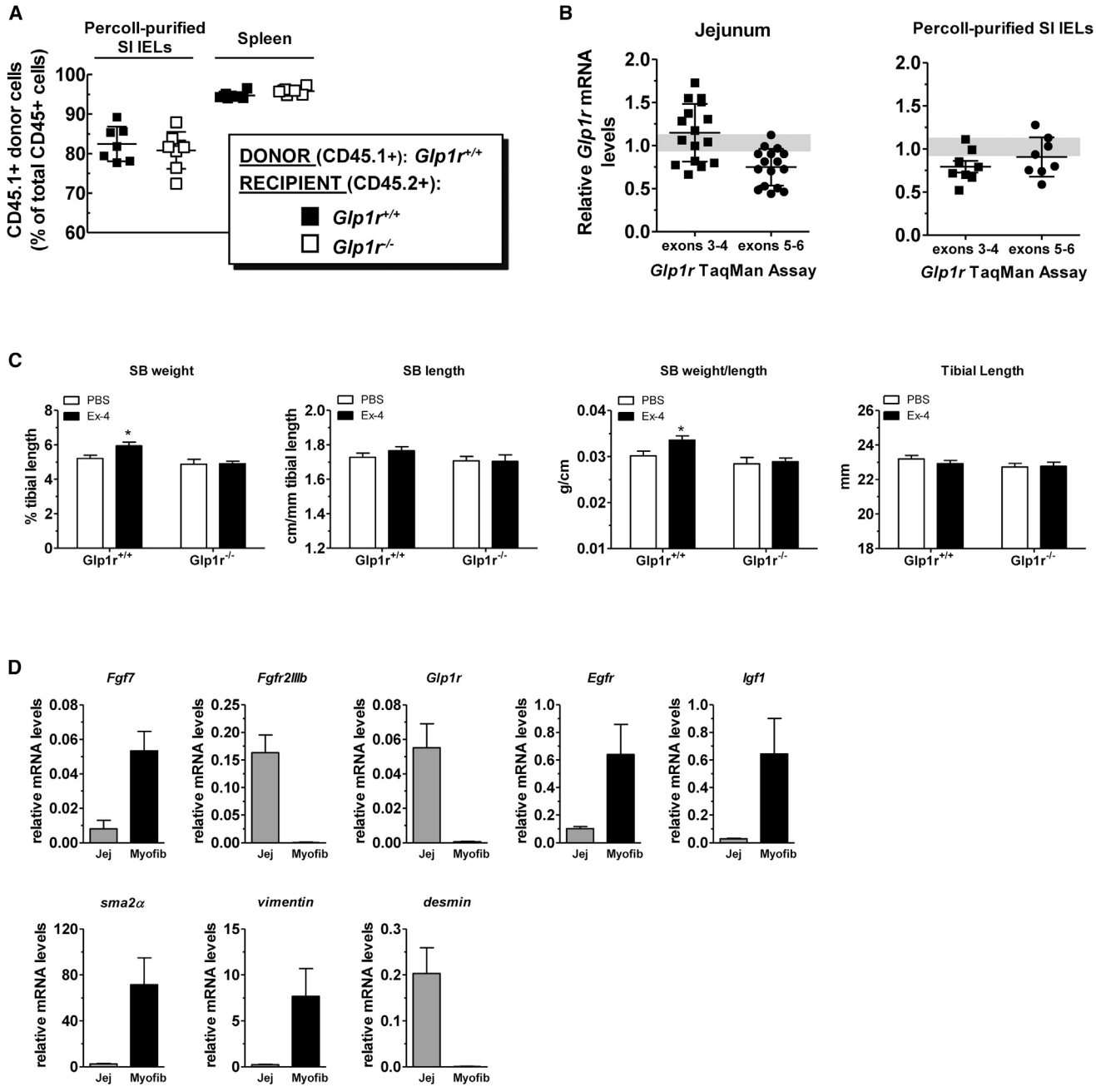

Figure 6. Ex-4 Does Not Increase Intestinal Weight in *Glp1r*$^{-/-}$ Mice following Reconstitution with *Glp1r*$^{+/+}$ IELs

(A) Donor chimerism in intestinal IELs and splenocytes of recipient *Glp1r*$^{+/+}$ and *Glp1r*$^{-/-}$ CD45.2^{+} male mice reconstituted with congenic bone marrow cells from *Glp1r*$^{+/+}$ CD45.1^{+} donor mice. Flow cytometry was performed on IELs isolated from the small intestine and splenocytes following staining with fluorescently labeled monoclonal antibodies (mAbs). Frequency is expressed relative to total CD45^{+} live events.

(B) Quantitative assessment of *Glp1r* expression in jejunum (left panel) and small intestinal IELs (right panel) of recipient *Glp1r*$^{-/-}$ male mice reconstituted with bone marrow from *Glp1r*$^{+/+}$ donor mice. The Taqman expression assay targeting exons 3–4 of the murine *Glp1r* mRNA detects both wild-type and knockout *Glp1r* transcripts, whereas the assay targeting exons 5–6 exclusively detects the wild-type *Glp1r* mRNA. *Glp1r* transcript levels are expressed relative to the *Glp1r* mRNA levels in *Glp1r*$^{+/+}$ recipient mice (gray horizontal stripe).

(C) Small bowel (SB) weight (as a percentage of tibia length), length (relative to tibia length), SB weight/unit length, and tibial length of recipient *Glp1r*$^{+/+}$ and *Glp1r*$^{-/-}$ mice 14–16 weeks after reconstitution treated with PBS or Ex-4 for 10 days. n = 8–10 males per group. Shown are combined data from two independent bone marrow transfer experiments. Data are means ± SE. *$p < 0.05$ versus PBS.

(D) qPCR analysis of RNA isolated from jejunum (Jej), or primary cultures of myofibroblasts (Myofib) prepared from mouse small intestine. Gene expression was assessed on cells at passage 3. Data are means ± SD from two independent experiments, comprised of two separate cultures, each derived from a separate mouse (n = 4 cultures).

treated with bariatric surgery revealed a significantly increased incidence of colorectal cancer, relative to obese control subjects (Derogar et al., 2013). Moreover, the incidence rate for development of colorectal cancer progressively increased with length of time after bariatric surgery (Derogar et al., 2013). However, the importance and mechanistic underpinning of these findings remains unclear and will require additional investigation.

Apc$^{Min/+}$ mice represent the most widely used genetically defined murine model for intestinal tumorigenesis and harbor a genetic mutation in the gene underlying the development of colon cancer in human subjects with familial adenomatous polyposis (Nishisho et al., 1991). Although the *Apc*$^{Min/+}$ mouse exhibits a propensity for small intestinal tumors and is an imperfect model for human colon cancer studies, loss of the APC tumor suppressor gene and activation of the Wnt/beta-catenin pathway are common genetic features of human colon cancer. Our data linking GLP-1R signaling to the control of murine gut growth may have translational implications for settings characterized by sustained elevations of levels of one or more intestinotrophic PGDPs in the treatment of metabolic disorders.

EXPERIMENTAL PROCEDURES

Reagents, Animals, and Treatments

Exendin-4 (Ex-4) was from Chi Scientific, liraglutide was from Novo Nordisk, the DPP-4-resistant analog human h[Gly^2]GLP-2 was from Pepceutical, recombinant mouse EGF was from Bachem, SAFE human recombinant KGF was from eBioscience, and tamoxifen was from MP Biomedicals. Peptides were dissolved in PBS (vehicle) and administered to mice by either intraperitoneal (i.p.) or subcutaneous (s.c.) injection at doses of Ex-4 (10 nmol/kg, BID), liraglutide (50 or 75 μg/kg, BID), h[Gly^2]GLP-2 (2.5 μg/mouse BID), or EGF (0.25 mg/kg, BID) unless otherwise specified. The doses of GLP-1R agonists employed were biologically active in the gut without producing significant weight loss. All animal experiments were approved by the Animal Care Committee of the Mount Sinai Hospital. Mice were bred at the Toronto Centre for Phenogenomics animal facility and were maintained on a standard diet and a 12 hr light/12 hr dark cycle.

C57BL/6J-*Apc*$^{Min/+}$, *Fgf7*$^{-/-}$ (B6.129-*Fgf7*^{tm1Efu}), *Egfr*$^{wa2/wa2}$ (*a/a Egfr*^{wa2}/J), and C57BL/6J mice were from The Jackson Laboratory. *Gcgr*$^{-/-}$ mice in the C57BL/6 background (Gelling et al., 2003) were crossed with *Glp1r*$^{-/-}$ (Scrocchi et al., 1996) or *Glp2r*$^{-/-}$ (Lee et al., 2012) mice in the same genetic background to generate *Gcgr*$^{+/-}$:*Glp1r*$^{+/-}$ or *Gcgr*$^{+/-}$:*Glp2r*$^{+/-}$ mice, which were bred to generate *Gcgr*$^{-/-}$:*Glp1r*$^{-/-}$ or *Gcgr*$^{-/-}$:*Glp2r*$^{-/-}$ and littermate controls. Male *Gcgr*$^{-/-}$:*Glp2r*$^{-/-}$ mice and age- and sex-matched littermate controls (n = 10–20) were approximately 36–38 weeks old at the time of sacrifice. Male *Gcgr*$^{-/-}$:*Glp1r*$^{-/-}$ and age- and sex-matched littermate controls (n = 9–13) were 20–22 weeks old at sacrifice. *Apc*$^{Min/+}$ mice were crossed with female *Glp1r*$^{-/-}$ mice to generate *Apc*$^{Min/+}$:*Glp1r*$^{+/-}$ and *Apc*$^{+/+}$:*Glp1r*$^{+/-}$ mice. Male *Apc*$^{Min/+}$:*Glp1r*$^{+/-}$ were bred with female *Apc*$^{+/+}$:*Glp1r*$^{+/-}$ to generate *Apc*$^{Min/+}$:*Glp1r*$^{+/+}$ and *Apc*$^{Min/+}$:*Glp1r*$^{-/-}$ mice. Investigators were blinded to genotype and treatment at the time of assessment.

Intestinal Growth

Unless otherwise indicated, non-fasted mice were euthanized by CO_2 inhalation the morning following the last injection (~12 hr after the last injection). Female *Glp1r*$^{-/-}$ and WT (*Glp1r*$^{+/+}$) littermate control mice (11 weeks old) were administered Ex-4 (s.c.) or PBS for 10 days, whereas male *Glp1r*$^{-/-}$ and WT (*Glp1r*$^{+/+}$) littermate control mice (11 weeks old) were administered liraglutide (75 μg/kg, i.p., BID) or PBS for 10 days. C57BL/6 male mice (11 weeks old) were administered exogenous Ex-4 (s.c.), h[Gly^2]GLP-2 (s.c.), both Ex-4 and h[Gly^2]GLP-2 (s.c.), or PBS for 10 days. Female *Egfr*$^{+/wa2}$ *and Egfr*$^{wa2/wa2}$ mice (8–12 weeks old) were treated with Ex-4 (i.p.) or PBS for 7 days. *Fgf7*$^{+/+}$ (WT) or *Fgf7*$^{-/-}$ mice (8–13 weeks old) were treated with Ex-4 (s.c.), h[Gly^2]GLP-2 (s.c.), or EGF (s.c.) for 10 days. IE-*Igf1r*KO mice were generated as described (Rowland et al., 2011). Cre recombinase was induced in mice aged 8–11 weeks by daily injection of tamoxifen (100 μl i.p., 10 mg/ml) for 5 days. Age- and sex-matched littermate *Igf1r*$^{flox/flox}$ and *villin-Cre-ER*$^{T2+/0}$ mice were controls and were also treated with tamoxifen. Approximately 24 hr after the final tamoxifen injection, mice were injected s.c. with PBS or liraglutide (50 μg/kg, BID) for 8 days. Mice were fasted overnight before sacrifice. See also Supplemental Experimental Procedures.

Glucose Tolerance Tests and Assessment of Gastric Emptying

Glucose tolerance (8–11 weeks old) and acetaminophen absorption (12–15 weeks old) tests to assess gastric emptying were carried out *Fgf7*$^{+/+}$ or *Fgf7*$^{-/-}$ mice as described (Lamont et al., 2012).

Statistical Analysis

Results are expressed as mean ± SE. Statistical significance was assessed by one-way or two-way ANOVA using Bonferroni's multiple comparison post test and, where appropriate, by unpaired Student's t test using GraphPad Prism 5 (GraphPad Software). Data were excluded from analysis if considered an outlier by the Grubbs' test (GraphPad Software). A p value < 0.05 was considered to be statistically significant.

ACCESSION NUMBERS

The NCBI GEO accession number for the microarray data reported in this paper is GSE63841.

SUPPLEMENTAL INFORMATION

Supplemental Information includes Supplemental Experimental Procedures, six figures, and one table and can be found with this article online at http://dx.doi.org/10.1016/j.cmet.2015.02.005.

AUTHOR CONTRIBUTIONS

J.A.K., L.L.B., B.Y., C.L., D.H., X.C., and K.J.R. planned and carried out experiments, analyzed results, and wrote and/or reviewed the manuscript. P.L.B. and D.J.D. planned experiments, analyzed results, and wrote the manuscript.

ACKNOWLEDGMENTS

These studies were supported in part by CIHR grants MOP 123391 and 12344, an operating grant from Novo Nordisk, the Canada Research Chairs Program, and a Banting and Best Diabetes Centre-Novo Nordisk Chair to D.J.D. D.J.D. has served as an advisor or consultant within the past 12 months to Arisaph Pharmaceuticals, Intarcia Therapeutics, Merck Research Laboratories, MedImmune, Novo Nordisk, NPS Pharmaceuticals, Receptos, Sanofi, and Transition Pharmaceuticals. Neither D.J.D. nor his family members hold stock directly or indirectly in any of these companies.

Received: July 22, 2014
Revised: December 9, 2014
Accepted: February 6, 2015
Published: March 3, 2015

REFERENCES

Ali, S., Lamont, B.J., Charron, M.J., and Drucker, D.J. (2011). Dual elimination of the glucagon and GLP-1 receptors in mice reveals plasticity in the incretin axis. J. Clin. Invest. *121*, 1917–1929.

Ali, S., Ussher, J.R., Baggio, L.L., Kabir, M.G., Charron, M.J., Ilkayeva, O., Newgard, C.B., and Drucker, D.J. (2015). Cardiomyocyte glucagon receptor signaling modulates outcomes in mice with experimental myocardial infarction. Molecular Metabolism *4*, 132–143.

Ashrafian, H., Ahmed, K., Rowland, S.P., Patel, V.M., Gooderham, N.J., Holmes, E., Darzi, A., and Athanasiou, T. (2011). Metabolic surgery and cancer: protective effects of bariatric procedures. Cancer *117*, 1788–1799.

Boismenu, R., and Havran, W.L. (1994). Modulation of epithelial cell growth by intraepithelial gamma delta T cells. Science *266*, 1253–1255.

Calle, E.E., and Thun, M.J. (2004). Obesity and cancer. Oncogene *23*, 6365–6378.

Campbell, J.E., and Drucker, D.J. (2013). Pharmacology, physiology, and mechanisms of incretin hormone action. Cell Metab. *17*, 819–837.

Chen, Y., Chou, K., Fuchs, E., Havran, W.L., and Boismenu, R. (2002). Protection of the intestinal mucosa by intraepithelial gamma delta T cells. Proc. Natl. Acad. Sci. USA *99*, 14338–14343.

Derogar, M., Hull, M.A., Kant, P., Östlund, M., Lu, Y., and Lagergren, J. (2013). Increased risk of colorectal cancer after obesity surgery. Ann. Surg. *258*, 983–988.

Drucker, D.J., and Yusta, B. (2014). Physiology and pharmacology of the enteroendocrine hormone glucagon-like peptide-2. Annu. Rev. Physiol. *76*, 561–583.

Drucker, D.J., Erlich, P., Asa, S.L., and Brubaker, P.L. (1996). Induction of intestinal epithelial proliferation by glucagon-like peptide 2. Proc. Natl. Acad. Sci. USA *93*, 7911–7916.

Drucker, D.J., Shi, Q., Crivici, A., Sumner-Smith, M., Tavares, W., Hill, M., DeForest, L., Cooper, S., and Brubaker, P.L. (1997). Regulation of the biological activity of glucagon-like peptide 2 in vivo by dipeptidyl peptidase IV. Nat. Biotechnol. *15*, 673–677.

Dubé, P.E., Forse, C.L., Bahrami, J., and Brubaker, P.L. (2006). The essential role of insulin-like growth factor-1 in the intestinal tropic effects of glucagon-like peptide-2 in mice. Gastroenterology *131*, 589–605.

Gelling, R.W., Du, X.Q., Dichmann, D.S., Romer, J., Huang, H., Cui, L., Obici, S., Tang, B., Holst, J.J., Fledelius, C., et al. (2003). Lower blood glucose, hyperglucagonemia, and pancreatic alpha cell hyperplasia in glucagon receptor knockout mice. Proc. Natl. Acad. Sci. USA *100*, 1438–1443.

Goodlad, R.A., Mandir, N., Meeran, K., Ghatei, M.A., Bloom, S.R., and Playford, R.J. (2000). Does the response of the intestinal epithelium to keratinocyte growth factor vary according to the method of administration? Regul. Pept. *87*, 83–90.

Greaves, L.C., Preston, S.L., Tadrous, P.J., Taylor, R.W., Barron, M.J., Oukrif, D., Leedham, S.J., Deheragoda, M., Sasieni, P., Novelli, M.R., et al. (2006). Mitochondrial DNA mutations are established in human colonic stem cells, and mutated clones expand by crypt fission. Proc. Natl. Acad. Sci. USA *103*, 714–719.

Grigoryan, M., Kedees, M.H., Charron, M.J., Guz, Y., and Teitelman, G. (2012). Regulation of mouse intestinal L cell progenitors proliferation by the glucagon family of peptides. Endocrinology *153*, 3076–3088.

Kant, P., Sainsbury, A., Reed, K.R., Pollard, S.G., Scott, N., Clarke, A.R., Coletta, P.L., and Hull, M.A. (2011). Rectal epithelial cell mitosis and expression of macrophage migration inhibitory factor are increased 3 years after Roux-en-Y gastric bypass (RYGB) for morbid obesity: implications for long-term neoplastic risk following RYGB. Gut *60*, 893–901.

Kedees, M.H., Guz, Y., Grigoryan, M., and Teitelman, G. (2013). Functional activity of murine intestinal mucosal cells is regulated by the glucagon-like peptide-1 receptor. Peptides *48*, 36–44.

Kissow, H., Hartmann, B., Holst, J.J., Viby, N.E., Hansen, L.S., Rosenkilde, M.M., Hare, K.J., and Poulsen, S.S. (2012). Glucagon-like peptide-1 (GLP-1) receptor agonism or DPP-4 inhibition does not accelerate neoplasia in carcinogen treated mice. Regul. Pept. *179*, 91–100.

Lai, G.Y., Park, Y., Hartge, P., Hollenbeck, A.R., and Freedman, N.D. (2013). The association between self-reported diabetes and cancer incidence in the NIH-AARP Diet and Health Study. J. Clin. Endocrinol. Metab. *98*, E497–E502.

Lamont, B.J., Li, Y., Kwan, E., Brown, T.J., Gaisano, H., and Drucker, D.J. (2012). Pancreatic GLP-1 receptor activation is sufficient for incretin control of glucose metabolism in mice. J. Clin. Invest. *122*, 388–402.

Lee, S.-J., Lee, J., Li, K.K., Holland, D., Maughan, H., Guttman, D.S., Yusta, B., and Drucker, D.J. (2012). Disruption of the murine Glp2r impairs Paneth cell function and increases susceptibility to small bowel enteritis. Endocrinology *153*, 1141–1151.

Li, C., Balluz, L.S., Ford, E.S., Okoro, C.A., Tsai, J., and Zhao, G. (2011). Association between diagnosed diabetes and self-reported cancer among U.S. adults: findings from the 2009 Behavioral Risk Factor Surveillance System. Diabetes Care *34*, 1365–1368.

Li, C.F., He, H.L., Wang, J.Y., Huang, H.Y., Wu, T.F., Hsing, C.H., Lee, S.W., Lee, H.H., Fang, J.L., Huang, W.T., and Chen, S.H. (2014). Fibroblast growth factor receptor 2 overexpression is predictive of poor prognosis in rectal cancer patients receiving neoadjuvant chemoradiotherapy. J. Clin. Pathol. *67*, 1056–1061.

Luetteke, N.C., Phillips, H.K., Qiu, T.H., Copeland, N.G., Earp, H.S., Jenkins, N.A., and Lee, D.C. (1994). The mouse waved-2 phenotype results from a point mutation in the EGF receptor tyrosine kinase. Genes Dev. *8*, 399–413.

Madsbad, S., Dirksen, C., and Holst, J.J. (2014). Mechanisms of changes in glucose metabolism and bodyweight after bariatric surgery. Lancet Diabetes Endocrinol *2*, 152–164.

Madsen, K.B., Askov-Hansen, C., Naimi, R.M., Brandt, C.F., Hartmann, B., Holst, J.J., Mortensen, P.B., and Jeppesen, P.B. (2013). Acute effects of continuous infusions of glucagon-like peptide (GLP)-1, GLP-2 and the combination (GLP-1+GLP-2) on intestinal absorption in short bowel syndrome (SBS) patients. A placebo-controlled study. Regul. Pept. *184*, 30–39.

Matsuda, Y., Ishiwata, T., Yamahatsu, K., Kawahara, K., Hagio, M., Peng, W.X., Yamamoto, T., Nakazawa, N., Seya, T., Ohaki, Y., and Naito, Z. (2011). Overexpressed fibroblast growth factor receptor 2 in the invasive front of colorectal cancer: a potential therapeutic target in colorectal cancer. Cancer Lett. *309*, 209–219.

Molina, J., Rodriguez-Diaz, R., Fachado, A., Jacques-Silva, M.C., Berggren, P.O., and Caicedo, A. (2014). Control of insulin secretion by cholinergic signaling in the human pancreatic islet. Diabetes *63*, 2714–2726.

Nilsson, R., Jain, M., Madhusudhan, N., Sheppard, N.G., Strittmatter, L., Kampf, C., Huang, J., Asplund, A., and Mootha, V.K. (2014). Metabolic enzyme expression highlights a key role for MTHFD2 and the mitochondrial folate pathway in cancer. Nat. Commun. *5*, 3128.

Nishisho, I., Nakamura, Y., Miyoshi, Y., Miki, Y., Ando, H., Horii, A., Koyama, K., Utsunomiya, J., Baba, S., and Hedge, P. (1991). Mutations of chromosome 5q21 genes in FAP and colorectal cancer patients. Science *253*, 665–669.

Ørskov, C., Hartmann, B., Poulsen, S.S., Thulesen, J., Hare, K.J., and Holst, J.J. (2005). GLP-2 stimulates colonic growth via KGF, released by subepithelial myofibroblasts with GLP-2 receptors. Regul. Pept. *124*, 105–112.

Otte, J.M., Schmitz, F., Banasiewicz, T., Drews, M., Fölsch, U.R., and Herzig, K.H. (2000). Expression of keratinocyte growth factor and its receptor in colorectal cancer. Eur. J. Clin. Invest. *30*, 222–229.

Panjwani, N., Mulvihill, E.E., Longuet, C., Yusta, B., Campbell, J.E., Brown, T.J., Streutker, C., Holland, D., Cao, X., Baggio, L.L., and Drucker, D.J. (2013). GLP-1 receptor activation indirectly reduces hepatic lipid accumulation but does not attenuate development of atherosclerosis in diabetic male ApoE(-/-) mice. Endocrinology *154*, 127–139.

Pathuri, G., Li, Q., Mohammed, A., Gali, H., Pento, J.T., and Rao, C.V. (2014). Synthesis and in vivo evaluation of N-ethylamino-2-oxo-1,2-dihydro-quinoline-3-carboxamide for inhibition of intestinal tumorigenesis in APC(Min/+) mice. Bioorg. Med. Chem. Lett. *24*, 1380–1382.

Plamboeck, A., Veedfald, S., Deacon, C.F., Hartmann, B., Wettergren, A., Svendsen, L.B., Meisner, S., Hovendal, C., Knop, F.K., Vilsbøll, T., and Holst, J.J. (2013a). Characterisation of oral and i.v. glucose handling in truncally vagotomised subjects with pyloroplasty. Eur. J. Endocrinol. *169*, 187–201.

Plamboeck, A., Veedfald, S., Deacon, C.F., Hartmann, B., Wettergren, A., Svendsen, L.B., Meisner, S., Hovendal, C., Vilsbøll, T., Knop, F.K., and Holst, J.J. (2013b). The effect of exogenous GLP-1 on food intake is lost in male truncally vagotomized subjects with pyloroplasty. Am. J. Physiol. Gastrointest. Liver Physiol. *304*, G1117–G1127.

Pyke, C., Heller, R.S., Kirk, R.K., Ørskov, C., Reedtz-Runge, S., Kaastrup, P., Hvelplund, A., Bardram, L., Calatayud, D., and Knudsen, L.B. (2014). GLP-1 receptor localization in monkey and human tissue: novel distribution revealed with extensively validated monoclonal antibody. Endocrinology *155*, 1280–1290.

Reimann, F., Tolhurst, G., and Gribble, F.M. (2012). G-protein-coupled receptors in intestinal chemosensation. Cell Metab. *15*, 421–431.

Richards, P., Parker, H.E., Adriaenssens, A.E., Hodgson, J.M., Cork, S.C., Trapp, S., Gribble, F.M., and Reimann, F. (2014). Identification and characterization of GLP-1 receptor-expressing cells using a new transgenic mouse model. Diabetes *63*, 1224–1233.

Rodriguez-Diaz, R., Dando, R., Jacques-Silva, M.C., Fachado, A., Molina, J., Abdulreda, M.H., Ricordi, C., Roper, S.D., Berggren, P.O., and Caicedo, A. (2011). Alpha cells secrete acetylcholine as a non-neuronal paracrine signal priming beta cell function in humans. Nat. Med. *17*, 888–892.

Rowland, K.J., Trivedi, S., Lee, D., Wan, K., Kulkarni, R.N., Holzenberger, M., and Brubaker, P.L. (2011). Loss of glucagon-like peptide-2-induced proliferation following intestinal epithelial insulin-like growth factor-1-receptor deletion. Gastroenterology *141*, 2166–2175, e7.

Sakthianandeswaren, A., Christie, M., D'Andreti, C., Tsui, C., Jorissen, R.N., Li, S., Fleming, N.I., Gibbs, P., Lipton, L., Malaterre, J., et al. (2011). PHLDA1 expression marks the putative epithelial stem cells and contributes to intestinal tumorigenesis. Cancer Res. *71*, 3709–3719.

Scrocchi, L.A., Brown, T.J., MaClusky, N., Brubaker, P.L., Auerbach, A.B., Joyner, A.L., and Drucker, D.J. (1996). Glucose intolerance but normal satiety in mice with a null mutation in the glucagon-like peptide 1 receptor gene. Nat. Med. *2*, 1254–1258.

Simonsen, L., Pilgaard, S., Orskov, C., Rosenkilde, M.M., Hartmann, B., Holst, J.J., and Deacon, C.F. (2007). Exendin-4, but not dipeptidyl peptidase IV inhibition, increases small intestinal mass in GK rats. Am. J. Physiol. Gastrointest. Liver Physiol. *293*, G288–G295.

Sjöström, L., Gummesson, A., Sjöström, C.D., Narbro, K., Peltonen, M., Wedel, H., Bengtsson, C., Bouchard, C., Carlsson, B., Dahlgren, S., et al.; Swedish Obese Subjects Study (2009). Effects of bariatric surgery on cancer incidence in obese patients in Sweden (Swedish Obese Subjects Study): a prospective, controlled intervention trial. Lancet Oncol. *10*, 653–662.

Snippert, H.J., Schepers, A.G., van Es, J.H., Simons, B.D., and Clevers, H. (2014). Biased competition between Lgr5 intestinal stem cells driven by oncogenic mutation induces clonal expansion. EMBO Rep. *15*, 62–69.

Terzić, J., Grivennikov, S., Karin, E., and Karin, M. (2010). Inflammation and colon cancer. Gastroenterology *138*, 2101–2114, e5.

Watanabe, M., Ishiwata, T., Nishigai, K., Moriyama, Y., and Asano, G. (2000). Overexpression of keratinocyte growth factor in cancer cells and enterochromaffin cells in human colorectal cancer. Pathol. Int. *50*, 363–372.

Wichmann, A., Allahyar, A., Greiner, T.U., Plovier, H., Lundén, G.O., Larsson, T., Drucker, D.J., Delzenne, N.M., Cani, P.D., and Bäckhed, F. (2013). Microbial modulation of energy availability in the colon regulates intestinal transit. Cell Host Microbe *14*, 582–590.

Yoshino, M., Ishiwata, T., Watanabe, M., Komine, O., Shibuya, T., Tokunaga, A., and Naito, Z. (2005). Keratinocyte growth factor receptor expression in normal colorectal epithelial cells and differentiated type of colorectal cancer. Oncol. Rep. *13*, 247–252.

Yusta, B., Holland, D., Koehler, J.A., Maziarz, M., Estall, J.L., Higgins, R., and Drucker, D.J. (2009). ErbB signaling is required for the proliferative actions of GLP-2 in the murine gut. Gastroenterology *137*, 986–996.

Zhang, J., Fan, J., Venneti, S., Cross, J.R., Takagi, T., Bhinder, B., Djaballah, H., Kanai, M., Cheng, E.H., Judkins, A.R., et al. (2014). Asparagine plays a critical role in regulating cellular adaptation to glutamine depletion. Mol. Cell *56*, 205–218.

Supplemental Experimental Procedures

Time course studies: Non-fasted male C57BL/6 mice (8-9 weeks-old) were injected sc with a single dose of Ex-4 (1 μg), EGF (0.5 mg/kg) or vehicle (PBS), and mice were killed 15, 30, 45, 60, or 90 min later by cervical dislocation. Alternatively, male C57BL/6 mice (11 weeks-old) were injected with Ex-4 for 4 h, or 24 h-7 days. Non-fasted mice were euthanized by CO_2 inhalation 4 h after the initial injection, or the morning following the last injection (~12 h after the last injection) for the 24 h-7 day time points. Blood samples were collected by cardiac puncture, chilled in the presence of 10% TED (v/v) (5000 kIU/ml Trasylol (Bayer), 1.2 mg/ml EDTA, and 0.1 nmol/l Diprotin A (Sigma Chemical Co., St. Louis, MO), and plasma was stored at -80°C.

Tissue collection, morphometry, immunohistochemistry, and polyp evaluation:

Following euthanasia, mice were weighed, the entire GI tract from the stomach to the rectum was removed, and gut weight and length was determined. Adjacent 2-cm intestinal segments from the SB and colon were fixed in 10% neutral-buffered formalin and paraffin embedded or snap-frozen in liquid nitrogen and stored at −70 ^{0}C. Tibial length was measured using an electronic caliper. To assess polyp burden, *Apc*$^{Min/+}$ and WT littermate control mice (6-9 week old) were administered exogenous Ex-4 or PBS for 4 weeks. Alternatively, 11 week old *Apc*$^{Min/+}$/*Glp1r*$^{+/+}$ and *Apc*$^{Min/+}$/*Glp1r*$^{-/-}$ littermate mice were assessed. The entire small intestine and colon were examined for polyps and for aberrant crypt foci (colon) as described (Koehler et al., 2008).

Immunohistochemistry and morphometry were done on 5-μm histological sections stained with hematoxylin and eosin (H&E) (Yusta et al., 2012). Sections were scanned using the Scanscope CS system (Aperio Technologies) at x20 magnification and digital images analyzed using Scanscope software (Aperio Technologies). The circumference surrounding the mucosa (encircling the area between the bottom of the crypts and the top of the submucosa) and the number of crypts/cross section were measured. To assess intestinal crypt cell proliferation, *Apc*$^{Min/+}$ and WT littermate control mice (8-12 weeks-old) were injected twice (3 h apart) with Ex-4, EGF (0.5 mg/kg, ip), or PBS followed by a single ip injection of 5-bromo-2′-deoxyuridine (BrdU) (Sigma-Aldrich; 100 mg/kg, dissolved in PBS) 1 h before death. BrdU immunopositivity and the incidence of BrdU staining at each cell position within the crypt were scored as described (Yusta et al., 2012). The level of apoptosis (TUNEL positive cells) or inflammation in SB polyps neutrophils (CL-8993AP, Cedarlane) was quantified.

Generation of Bone Marrow Chimeras, Isolation of Mouse Intestinal Intraepithelial Lymphocytes (IELs) and Splenocytes, and Myofibroblast Cultures:

Bone marrow chimeras were generated by lethally irradiating *Glp1r*$^{+/+}$ or *Glp1r* $^{-/-}$ CD45.2^{+} recipient male mice (1100 cGy, split into two equal doses administered 4 hours apart) followed by tail vein injection of 5 x 10^6 congenic bone marrow cells from donor WT (*Glp1r*$^{+/+}$) CD45.1^{+} male mice administered as described (Auletta et al., 2004). Fourteen to sixteen weeks after bone marrow transplant, mice were treated with vehicle or Ex-4 for 10 days, sacrificed, and analyzed for intestinal growth. Chimerism was assessed by 1) flow cytometry on IELs isolated from the small intestine and splenocytes following staining with fluorescently labelled mAbs against CD45, and 2) quantitative PCR analysis using primers that differentiate between *Glp1r*$^{+/+}$ and *Glp1r*$^{-/-}$ transcripts using RNA isolated from recipient jejunum and sorted IELs. Murine

intestinal IELs were obtained following established protocols (Lefrancois and Lycke, 2001). Mouse splenocytes were isolated by mechanical dissociation of the spleen followed by red blood cell lysis. Primary cultures of myofibroblasts were prepared from mouse small intestine as described (Shaker et al., 2010). Gene expression was assessed on cells at passage 3.

RNA isolation, quantitative real-time RT-PCR, Southern and Western blot analysis:

Human colorectal tumors and adjacent normal tissue were obtained from the Mount Sinai Hospital tissue bank, following research ethics approval. Real-time quantitative PCR was performed on an ABI PRISM 7900HT Sequence Detection System (Applied Biosystems, Foster City, CA) with TaqMan Universal PCR Master Mix and TaqMan Gene Expression Assays (Applied Biosystems). Relative values for mRNA transcripts (quantified by by the $2^{-\Delta Ct}$ method) were normalized to the mRNA levels of cyclophillin (*Ppia*). Values for mRNA transcripts in $Apc^{Min/+}$ and WT littermate mice after 6 h treatment with Ex-4 were normalized to GAPDH mRNA levels. *Glp1r* mRNA expression in colon polyps from $Apc^{Min/+}$ mice was detected by RT-PCR and Southern blot analysis (Hadjiyanni et al., 2008). CT26 colon cancer RNA was used as a positive control (Koehler et al., 2011).

Whole-tissue extracts were prepared by homogenization of intestinal segments (2 cm) in ice-cold RIPA buffer (1% Nonidet P-40, 0.5% sodium deoxycholate, and 0.1% sodium dodecyl sulfate in Tris-buffered saline) supplemented with protease and phosphatase inhibitors (Sigma-Aldrich), 5 mmol/L sodium flouride, 5 mmol/L β-glycerophosphate, and 200 μmol/L sodium orthovanadate. Protein (30–45 μg) was used for Western blot analysis. The antibodies phospho-Erk1/2 (Thr-202/Tyr-204, 9101), phospho-Akt (Ser-473, 9271), phospho-GSK3a/b (Ser-21/9, 9331), phospho-IkB (Ser-32, 9241), phospho-Jun (Ser-73, 9164), phospho-STAT3 (Tyr705,

M9C6), and YAP (4912) were from Cell Signaling Technologies, Beverly, MA and used at a 1:1000 dilution. A mouse monoclonal antibody against heat-shock protein 90 (BD Biosciences, Mississauga, Ontario, Canada, 610418) was used as a loading control at a 1:2000 dilution. Phospho-c-myc (Ser-62, ab51156) was from Abcam, Cambridge, MA and used at a 1:1000 dilution. c-myc (9E10) was from Santa Cruz Biotechnologies (1:1000) , Santa Cruz, CA.

Microarray Analysis:

Non-fasted male C57BL/6 mice (11-12 weeks-old) were injected with a single dose of Ex-4 or KGF (1 mg/kg) and sacrificed 1, 5 or 20 h later by CO_2 inhalation. RNA was isolated from mucosal scrapings taken from a 2 cm piece of the jejunum. Microarray analysis was performed (www.pmgenomics.ca) using the Illumina Mouse Whole Genome (WG-6V2) Beadchip. See also Supplemental Experimental Procedures. The accession number for the microarray data is GSE63841. Data was checked for overall quality using R (v3.0.2) with the Bioconductor framework and the LUMI package. Data was then imported in GeneSpring v12.6.1 for analysis. During import, the data was normalized using a standard (for Illumina arrays) quantile normalization followed by a "per probe" median centered normalization. All data analysis and visualization were performed on log2 transformed data. A total of 45,281 probes are represented on the Mouse WG-6 Beadchip. Data was first filtered to remove the confounding effect probes that show no signal may have on subsequent analysis. Only probes that were above the 20th percentile of the distribution of intensities in 100% of any of the 1 of 3 groups (control, Ex-4, KGF) were allowed to pass through this filtering. A one way ANOVA with a p value cut off of 0.05 was performed followed by a post-hoc Tukey's HSD test to generate sets of post-hoc significant FDR corrected probes for each specific comparison of interest (ie control vs Ex4 or Fgf7/KGF). VENN Diagrams (http://bioinfogp.cnb.csic.es/tools/venny) were then created to

compare the treatments after dividing the post-hoc results into fold change of at least 1.2 up or down.

Auletta, J.J., Devecchio, J.L., Ferrara, J.L., and Heinzel, F.P. (2004). Distinct phases in recovery of reconstituted innate cellular-mediated immunity after murine syngeneic bone marrow transplantation. Biology of blood and marrow transplantation : journal of the American Society for Blood and Marrow Transplantation 10, 834-847.
Hadjiyanni, I., Baggio, L.L., Poussier, P., and Drucker, D.J. (2008). Exendin-4 modulates diabetes onset in nonobese diabetic mice. Endocrinology 149, 1338-1349.
Koehler, J.A., Harper, W., Barnard, M., Yusta, B., and Drucker, D.J. (2008). Glucagon-like peptide-2 does not modify the growth or survival of murine or human intestinal tumor cells. Cancer research 68, 7897-7904.
Koehler, J.A., Kain, T., and Drucker, D.J. (2011). Glucagon-like peptide-1 receptor activation inhibits growth and augments apoptosis in murine CT26 colon cancer cells. Endocrinology 152, 3362-3372.
Lefrancois, L., and Lycke, N. (2001). Isolation of mouse small intestinal intraepithelial lymphocytes, Peyer's patch, and lamina propria cells. Current protocols in immunology / edited by John E. Coligan ... [et al.] Chapter 3, Unit 3 19.
Shaker, A., Swietlicki, E.A., Wang, L., Jiang, S., Onal, B., Bala, S., DeSchryver, K., Newberry, R., Levin, M.S., and Rubin, D.C. (2010). Epimorphin deletion protects mice from inflammation-induced colon carcinogenesis and alters stem cell niche myofibroblast secretion. The Journal of clinical investigation 120, 2081-2093.
Yusta, B., Holland, D., Waschek, J.A., and Drucker, D.J. (2012). Intestinotrophic glucagon-like peptide-2 (GLP-2) activates intestinal gene expression and growth factor-dependent pathways independent of the vasoactive intestinal peptide gene in mice. Endocrinology 153, 2623-2632.

Figure S1:

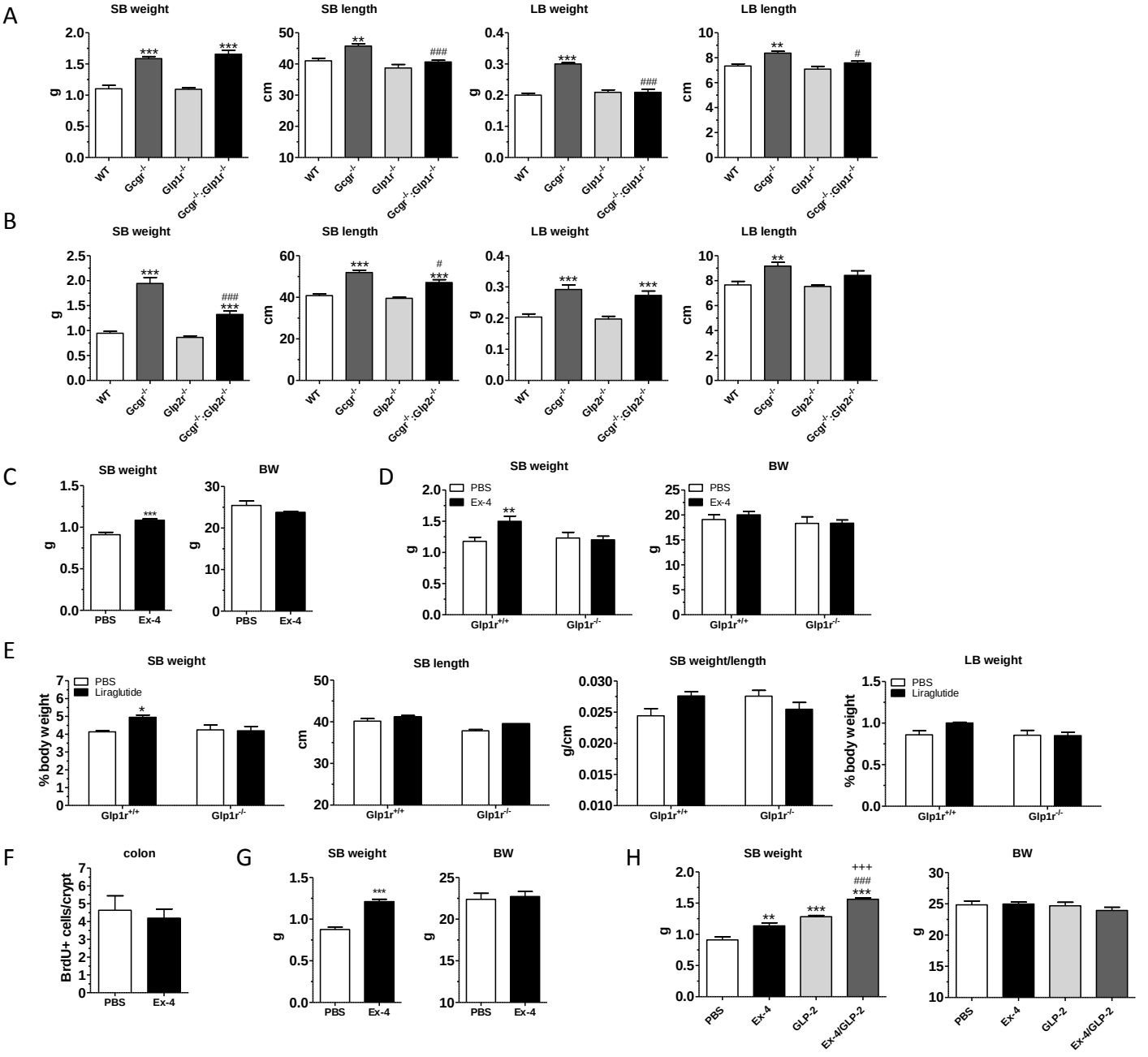

Figure S1, Related to Figure 1: (A-B) Small bowel (SB) and large bowel (LB) weight and length of male (A) *Glp1r*$^{-/-}$ and *Gcgr*$^{-/-}$:*Glp1r*$^{-/-}$ or (B) *Glp2r*$^{-/-}$ and *Gcgr*$^{-/-}$:*Glp2r*$^{-/-}$ mice and wild-type (WT) and *Gcgr*$^{-/-}$ littermate control mice. n=9-13 (A) or n=10-20 (B) mice per group. Data are means ± SE ** p<0.01, *** p<0.001 vs WT mice, # p<0.05, ### p<0.001 vs *Gcgr*$^{-/-}$ mice. (C-D) Absolute SB weights and body weights of (C) C57BL/6 male mice following administration of Ex-4 or vehicle (PBS) for 7 days. n=5 in each group, or (D) female *Glp1r*$^{-/-}$ and *Glp1r*$^{+/+}$ littermate control mice administered Ex-4 or PBS for 10 days. n=4-6 mice per group. (E) SB and LB weight (as a % of body weight), and SB length and weight/unit length of female *Glp1r*$^{-/-}$ and *Glp1r*$^{+/+}$ littermate control mice administered liraglutide or PBS for 10 days. n=3 in each group. (F) BrdU labeling in the colon crypt compartment of WT mice after 2 injections (3 hours apart) of Ex-4 or PBS, followed by a 1 h pulse with BrdU. Schematic representation of the experimental design is shown *Fig 1C*. Tissue sections were scored for total number of BrdU+ cells per crypt from at least 20 well-oriented crypts/mouse. Data are means ± SE. n=6 from two experiments. (G-H) Absolute SB weights and body weights of (G) WT male mice administered exogenous Ex-4 or PBS for 4 weeks. n=10 in each group from three experiments. (H) C57BL/6 male mice following administration of PBS, Ex-4, Gly2-GLP-2 (GLP-2), or both Ex-4 and Gly2-GLP-2 (Ex 4/GLP-2) for 10 days. n=5 in each group . For C-H, data are means ± SE *p<0.05 ** p<0.01 *** p<0.001 *vs.* PBS. ### p<0.001 Ex-4 *vs* Ex-4+Gly2-GLP-2, +++ p<0.001 Gly2-GLP-2 *vs* Ex-4+ Gly2-GLP-2.

Figure S2:

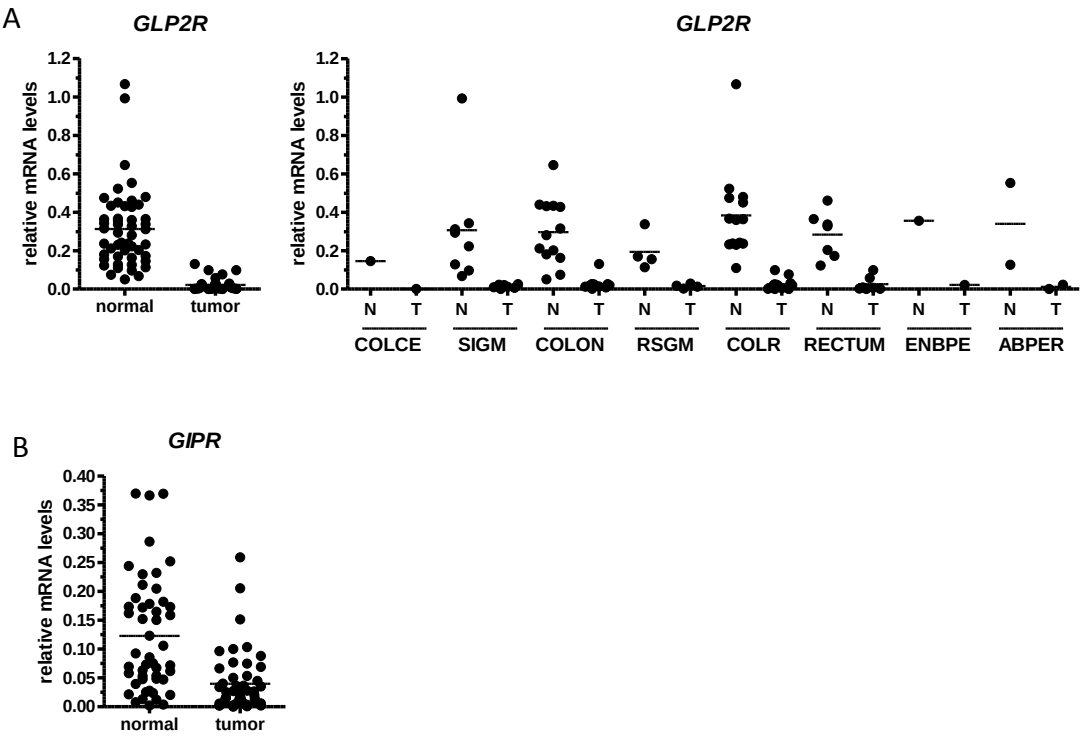

Figure S2, Related to Figure 2: Both normal colon and colon tumor samples from 50 patients with colorectal cancer were assessed for (A) *GLP2R* or (B) *GIPR* expression by qPCR. (A) *Right panel*: relative *GLP2R* mRNA levels in normal colon (N) and tumor (T) samples designated and graphed according to tumor location. Colce (colon/cecum--proximal colon), SGM (sigmoid colon--distal region before rectum), Colon, RSGM (rectosigmoid), COLR (colorectal), Rectum, ENBPE (en-bloc peritoneum), ABPER (abdominal peritoneal).

Figure S3:

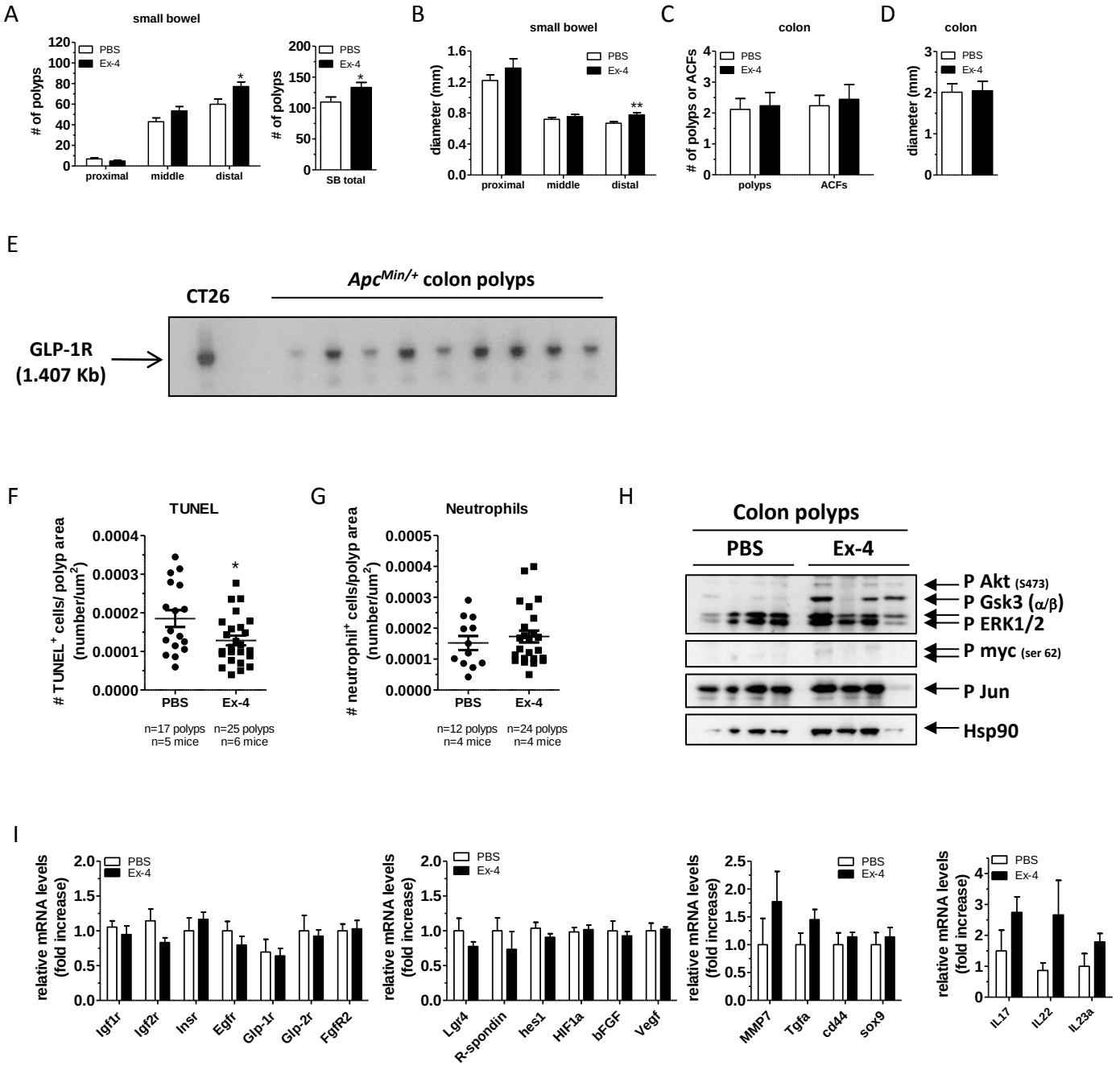

Figure S3, Related to Figure 2: *Apc*$^{Min/+}$ mice were administered exogenous Ex-4 or vehicle (PBS) for 4 weeks. Number (A) and size (B) of polyps in the different sections of the small bowel or total number of polyps in entire small bowel (SB; A, *right panel*) of male *Apc*$^{Min/+}$ mice. Number of polyps and aberrant crypt foci (ACF) (C) and size of polyps (D) in the colons of male *Apc*$^{Min/+}$ mice. n=15 mice for each group. Data are means ± SE. * p<0.05, ** p<0.01 *vs* PBS. (E) RT-PCR and Southern blot analysis for the *Glp1r* in colon polyps from *Apc*$^{Min/+}$ mice. Each lane represents a single polyp from separate mice . (F-G) Number of TUNEL positive cells (F) or neutrophils (G) in SB polyps of *Apc*$^{Min/+}$ mice treated with Ex-4 or PBS for 1 week. Shown are the number of positive cells per polyp area for each individual polyp quantified. Means ± SE are also indicated. * p<0.05 *vs* PBS. Total number of polyps and the number of mice used in the analysis are shown underneath. (H) Western blot analysis of colon polyps of *Apc*$^{Min/+}$ mice treated as indicated in Fig 2K. Each lane represents a single polyp from a separate mouse. (I) qPCR analysis of colon polyps of *Apc*$^{Min/+}$ mice treated with PBS or Ex-4 for 4 weeks. n=5 or 8 in each group. Data are means ± SE from three experiments.

Figure S4:

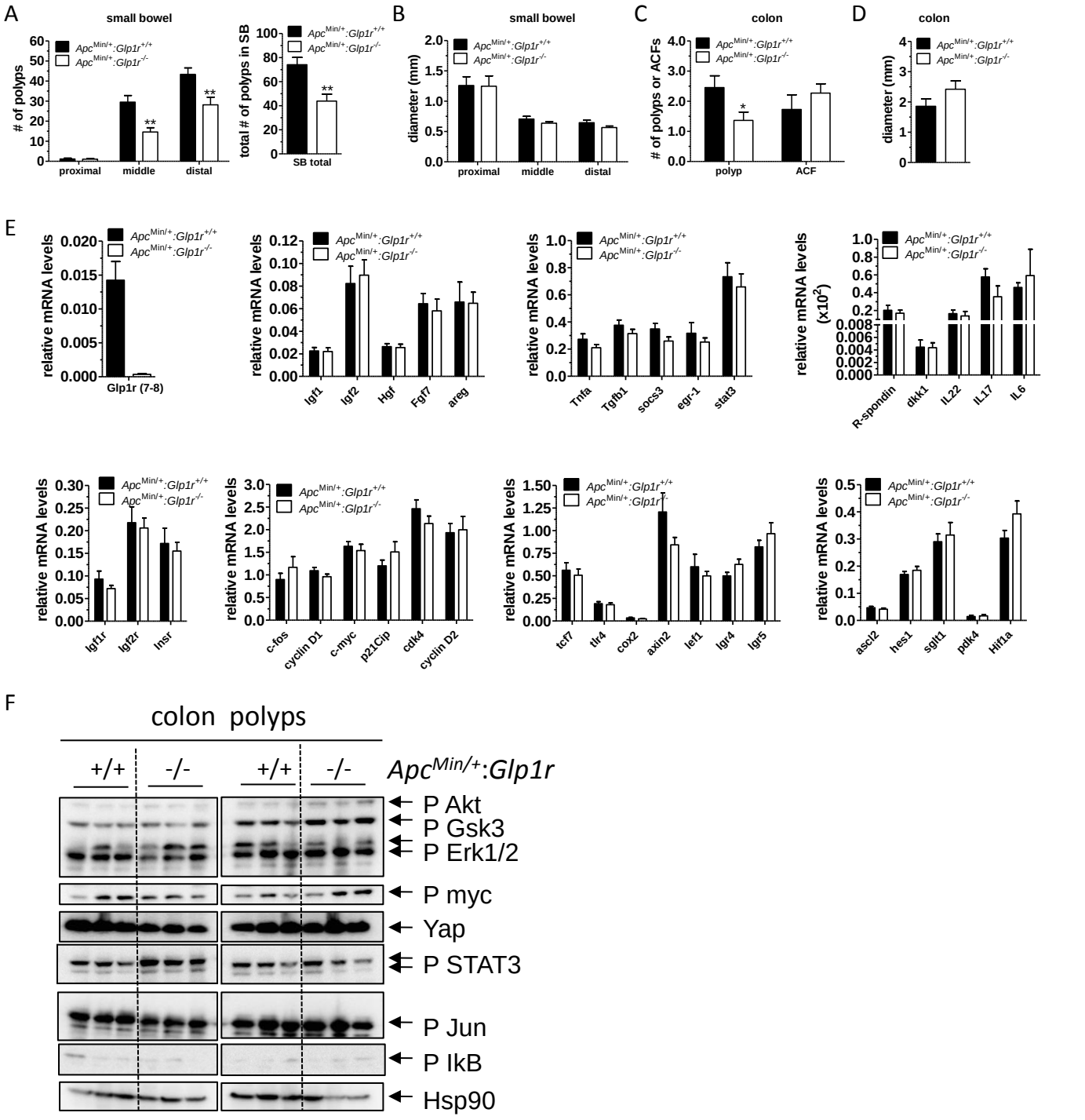

Figure S4, Related to Figure 2: Number (A) and size (B) of polyps in the different sections of the small bowel, or total number of polyps in entire small bowel (SB; A, *right panel*) of male *Apc*$^{Min/+}$:*Glp1r*$^{+/+}$ and littermate *Apc*$^{Min/+}$:*Glp1r* $^{-/-}$ mice. The number of polyps and aberrant crypt foci (ACF) (C) and size of polyps (D) that developed in the colons of male *Apc*$^{Min/+}$:*Glp1r*$^{+/+}$ and littermate *Apc*$^{Min/+}$:*Glp1r* $^{-/-}$ mice. n=11 for all genotypes. Data are means ± SE. * p<0.05, ** p<0.01 *vs Apc*$^{Min/+}$:*Glp1r* $^{+/+}$ mice. (E) mRNA levels of the indicated transcripts were determined by quantitative RT-PCR in total RNA from colon polyps of *Apc*$^{Min/+}$:*Glp1r*$^{+/+}$ and *Apc*$^{Min/+}$:*Glp1r* $^{-/-}$ mice. Data are means ± SE n=8 for each genotype. (F) Western blot analysis of colon polyps from *Apc*$^{Min/+}$:*Glp1r*$^{+/+}$ and *Apc*$^{Min/+}$:*Glp1r* $^{-/-}$ mice. Each lane represents a single polyp from separate mice.

Figure S5:

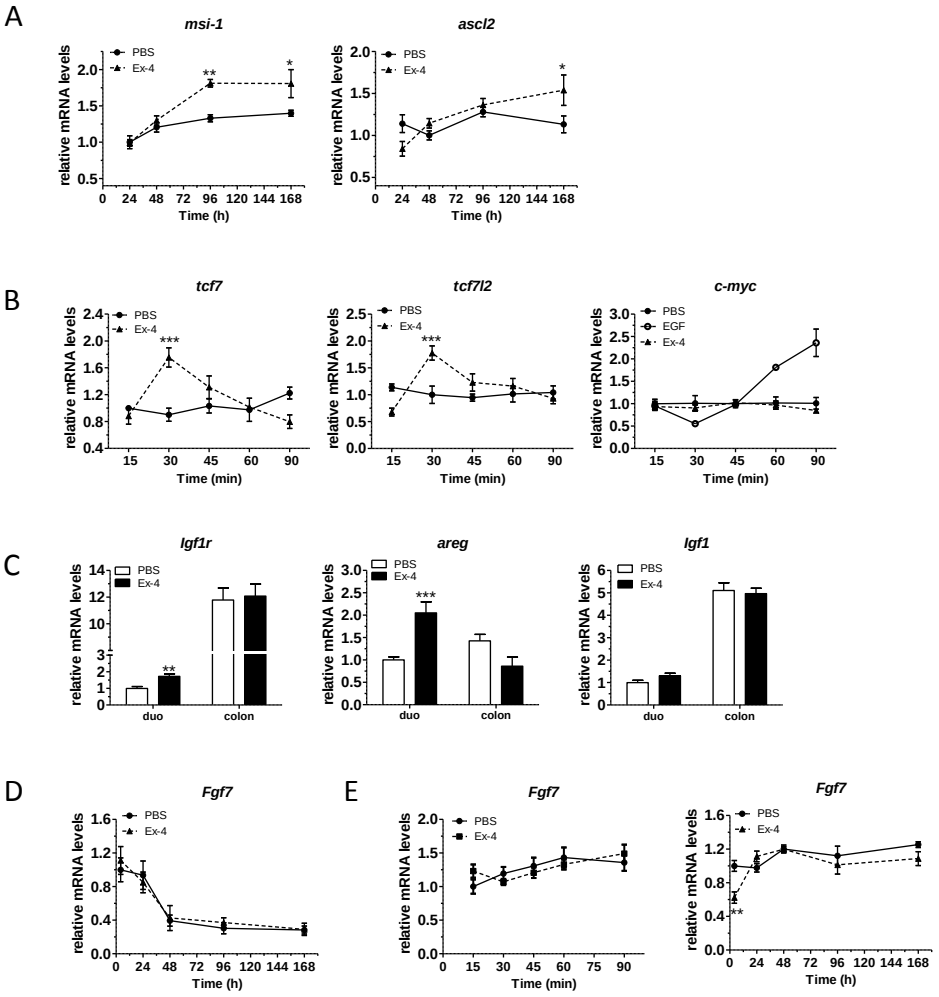

Figure S5, Related to Figures 3 and 4: (A-B) qPCR analysis of RNA isolated from jejunum of male C57BL/6 mice treated with (A) Ex-4 for 1-7 days, or (B) 15-90 min after a single injection of Ex-4, EGF or PBS. (A) n=5, or (B) n=4 mice in each group. (C) qPCR analysis of RNA from duodenum and colon of WT littermates of *Apc*$^{Min/+}$ mice 6 h after injection with Ex-4 or PBS. n = 6 in each group. (D) qPCR analysis of RNA isolated from jejunum of male C57BL/6 mice treated with Ex-4 or PBS for 4 h-7 days. n=5 mice per group. (E) qPCR analysis of RNA isolated from colon of male C57BL/6 mice at 15-90 min after a single injection of Ex-4 or PBS (*left panel*) n=4 mice per group, or treated with Ex-4 or PBS for 4 h-7 days (*right panel*) n=5 mice per group. For A-E, results are expressed as means ± SE. *p<0.05, ** p<0.01, *** p<0.001 *vs* PBS.

Figure S6:

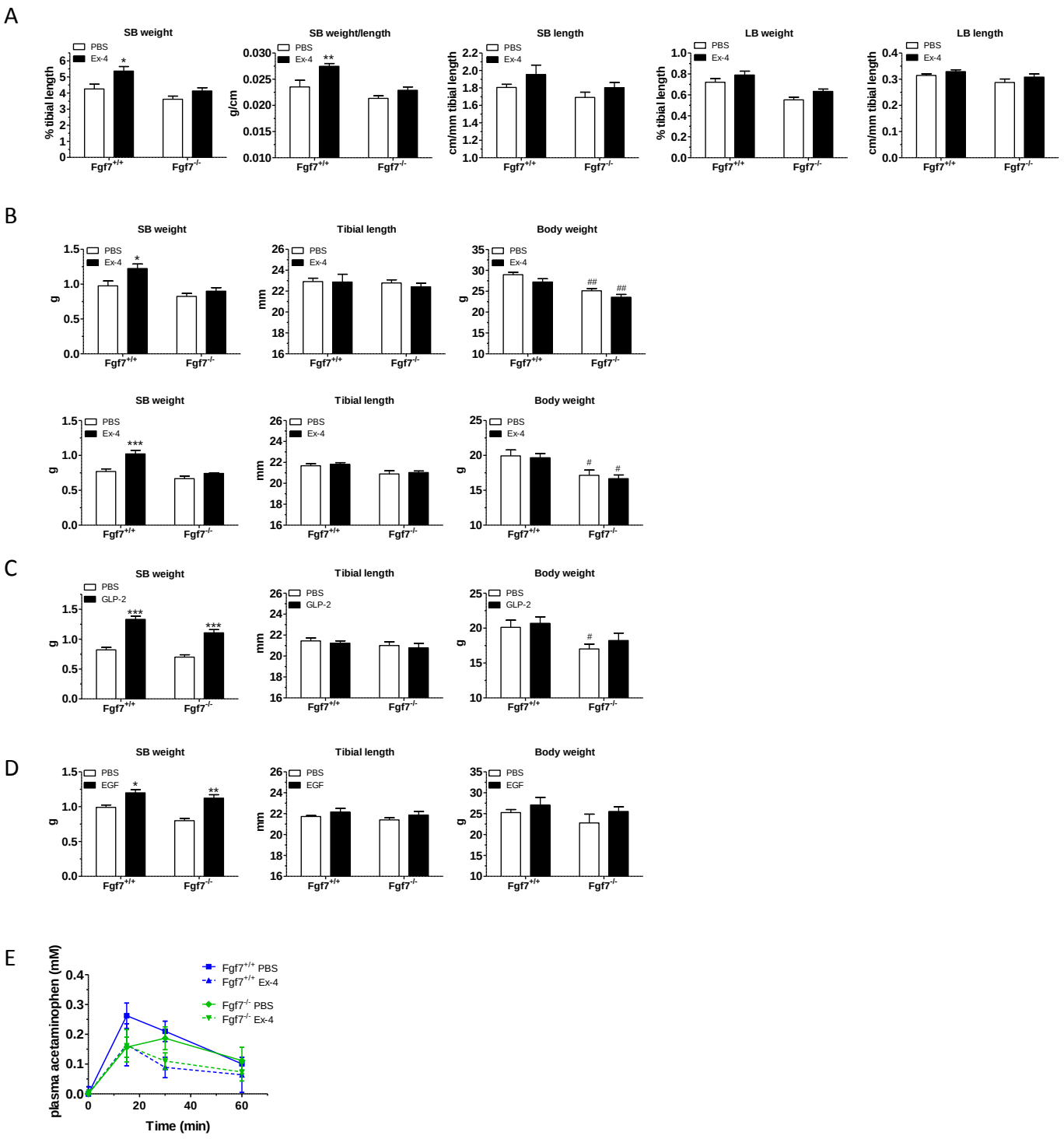

Figure S6, Related to Figure 4: (A) small bowel (SB) and large bowel (LB) weight (as a % of tibia length), length (relative to tibial length) and SB weight/unit length of *Fgf7* $^{+/+}$ or *Fgf7* $^{-/-}$ male mice treated with PBS or Ex-4 for 10 days. n= 4-5 mice in each group. Data are means ± SE. *p<0.05, ** p<0.01 *vs* PBS. (B-D) Absolute small bowel (SB) weight, tibial length, and body weights of *Fgf7* $^{+/+}$ or *Fgf7* $^{-/-}$ mice treated for 10 days with PBS or : (B) Ex-4 (*upper panels*, n= 4-5 males per group)(*lower panels*, n=6-8 females per group), (C) Gly2-GLP-2 (n=5-6 females per group), or (D) EGF (n=3-4 males per group). Data are means ± SE * p<0.05, ** p<0.01 *** p<0.001 *vs* PBS, # p<0.05 ## p<0.01 *Fgf7* $^{+/+}$ *vs Fgf7* $^{-/-}$ mice. (E) The appearance of acetaminophen in plasma samples was used to measure gastric emptying in *Fgf7* $^{-/-}$ and *Fgf7* $^{+/+}$ littermate control mice treated with PBS or Ex-4. n=3-5 mice per group.

Table S1:

Summary of qPCR analysis of WT mice:

- : no change, ND: not determined

acute time course (15-90 min)			chronic time course (4h-7 days)			6 h time point		
C57Bl6J			C57Bl6J			WT littermates of *Apc*$^{Min/+}$ mice		
gene	**jej**	**colon**	**gene**	**jej**	**colon**	**gene**	**duo**	**colon**
Fgf7 (*Kgf*)	↑	–	*Fgf7*	–	↓ 4 h	*Fgf7*	↑	↓
Igf1	–	↑ 30 min	*Igf1*	↑ 4 h	↑ 4 h ↓48 h	*Igf1*	–	–
Igf2	ND	–	*Igf2*	–	–	*Igf2*	–	–
areg	–	–	*areg*	↑ 4 h	–	*areg*	↑	–
ereg	–	–	*ereg*	↑ 4 h	–	*ereg*	–	–
HB-Egf	–	–						
tcf7	↑ 30 min	ND	*tcf7*	–	–	*tcf7*	–	–
tcf7 l2	↑ 30 min	ND	*axin2*	–	↓ 96 h			
c-myc	–	–	*c-myc*	↑ 4 h	–	*c-myc*	↑	–
c-fos	–	–	*c-fos*	–	↓ trend, not sig	*c-fos*	–	↓
egr-1	–	–	*egr-1*	↑ 4 h	–	*egr-1*	–	–
wnt5a	–	ND	*c-jun*	–	–	*c-jun*	–	–
jag	↑ 30 min	ND	*jag*	–	ND	*jag*	–	–
hes	–	ND	*hes*	–	ND	*hes*	–	–
olfm4	–	ND	*olfm4*	–	–			
msi-1	↑ 30 min	ND	*msi-1*	↑4 d , 7d	–			
			ascl2	↑7 d	–	*ascl2*	–	–
R-spondin	–	ND	*R-spondin*	↓ trend, not sig	–	*R-spondin*	↓	↓
			Lgr5	–	↓ 48 h	*Lgr5*	–	–
sox9	–	–	*sox9*	↑4 d				
Phlda 1	–	–						
p21cip	ND	–						
			Socs3	↑ 4 h	↑ 4 h	*Socs3*	↑	↑
			Stat3	–	–	*Stat3*	–	–
			Hgf	↑ 4 h	↓ 7 days	*Hgf*	–	–
						Tgfb1	–	–
			Egf	–	–			
						Hif1a	–	–
			cyclin D1	–	–	*cyclin D1*	–	–
						cyclin D2	–	–
			cdk4	–	–	*cdk4*	–	–
						p21cip	–	–
			cox2	↑ 4 h	–	*cox2*	–	–
						Cd44	–	↓
						Insr	–	–
						Fgfr2	–	–
			EphB2	–	–	*Egfr*	–	–
						Igf1r	↑	–
			Glut2	↓ 4 h	–	*Glut2*	–	–
						Glut5	–	↑(very low)
			Sglt1	–	↑ 4 h			

Summary of qPCR analysis of *Apc*$^{Min/+}$ mice:

- : no change, ND: not determined

30 min time point				6 h time point		
Apc$^{Min/+}$ mice				*Apc*$^{Min/+}$ mice		
gene	**duo**	**colon**	**colon polyps**	**gene**	**duo**	**colon**
Fgf7	–	–	↑ 30 min	*Fgf7*	–	–
Igf1	–	↓ 30 min	–	*Igf1*	–	–
Igf2	–	–	–	*Igf2*	–	–
areg	–	–	–	*areg*	↑	↓
ereg	–	–	↑	*ereg*	–	–
tcf7	–	–	–	*tcf7*	–	–
c-myc	↑	–	–	*c-myc*	–	↑
				c-fos	–	↓
egr-1	–	–	–	*egr-1*	–	–
				c-jun	–	–
Socs3	–	–	↑	*Socs3*	↑	↑
				Stat3	–	–
Hgf	–	–	–	*Hgf*	–	–
Tgfb1	–	–	–	*Tgfb1*	↑	↓
cyclin D1	–	–	–	*cyclin D1*	–	–
cyclin D2	–	–	–	*cyclin D2*	–	–
cdk4	–	–	–	*cdk4*	–	–
p21cip	–	–	–	*p21cip*	–	–
cox2	–	–	–	*cox2*	–	–
				Cd44	–	↓
				Insr	–	–
				Fgfr2	–	–
				Egfr	↑	–
				Igf1r	↑	–
				Glut2	–	–
				Glut5	–	↑(very low)

Table S1, Related to Figures 2-4: Summary of all genes examined at the indicted time points for both acute and chronic time course studies in C57BL/6 mice, and *Apc*$^{Min/+}$ and WT littermate control mice. ↑ and ↓ arrows indicated a significant increase, or decrease in gene expression (or trend where indicated), respectively, by Ex-4 *vs* control. (-) indicates no change (ND): not determined